University of Alberta

Functional Imaging of Cancer Mitochondria with Multiphoton Confocal Microscopy

By

Alois Stephan Haromy

A thesis submitted to the Faculty of Graduate Studies and Research
in partial fulfillment of the requirements for the degree of

Master of Science
in
Experimental Medicine

Medicine

Spring 2012
Edmonton, Alberta

Dedication

I wish to dedicate this thesis to my dear departed parents.
Although, unfortunately neither of them lived to see the completion of this work, the love, encouragement and support, which they offered me over the years in all my endeavors, gave me the drive and incentive to strive for this goal even when circumstances made it seem as if any chance to attain it was long passed. Even so, they never stopped believing in my abilities and for this they will have my everlasting gratitude.

Abstract

Maximizing the possibility of effectively treating cancer requires timely assessment of its aggressiveness and susceptibility to drug intervention. During cancer surgery, the "fast biopsy" is a commonly employed technique to assess a tumor's invasiveness and guide surgery. Unfortunately, it is of limited value in predicting a tumor's metastatic potential and susceptibility to drug treatment. However, certain functional biomarkers, like mitochondrial membrane potential and reactive oxygen species, which may be indicative of both aggressiveness and drug susceptibility, can be measured in "real time" using confocal microscopy. To this end, theoretical and practical aspects of functional confocal imaging are presented as a general overview and in conjunction with a clinical trial treating glioblastoma multiforme (GBM) using the metabolic modulating drug DCA. Functional imaging of biopsies from 40 GBM patients, various cancer and normal cell lines validated confocal microscopy as a tool assessing functional biomarkers and the effectiveness of DCA treatment.

Acknowledgements

Special Thanks to:

•My supervisor **Dr. Evangelos Michelakis**, for allowing me valuable lab time while I completed my experiments and whose patient mentorship and assistance over the past 6 years was invaluable for the completion of this thesis and my program of studies.

•**Gopinath Sutendra** whose valuable suggestions and input contributed immeasurably to the final completion of this work.

•**Peter Dromparis** whose useful suggestions and whose assistance with the GBM tissue staining and experiments were of vital importance.

•**Roxane Paulin** whose timely assistance with the final formatting and polishing of the draft saved me uncounted hours of trial and error.

•**Sandra Bonnet** who performed the initial work in trouble shooting the culturing and DCA treatment of the cancer cell lines and who assisted in the TMRM Mitosox experiments.

•The other members of our lab (lab manager **Kyoko Hashimoto**) and those former and current technicians who contributed in various diverse ways.

•**The Division of Neurosurgery** of the University of Alberta Hospital

•My examining committee:
Dr. Evangelos Michelakis, **Dr. Sean McMurtry,**
Dr. Ying Tsui and Chairman Dr. Ross Tsuyuki.

TABLE OF CONTENTS

LIST OF TABLES

LIST OF FIGURES

Introduction

The objective of this thesis is to:

a) Present a general review of the basic physics and optics of multiphoton confocal microscopy with an emphasis on functional imaging of mitochondria in living cells. This represents more than 12 years of experience with confocal microscopy and aims to bring up practical concepts, principles and challenges in the reliable utilization of this technique particularly when used in medical decision making and drug discovery programs.

b) Present a series of experiments using this technique in studies of mitochondrial function in freshly extracted human tumors (glioblastoma multiforme, GBM) as well as in a number of cancer cell lines. Given the importance of mitochondria in the "metabolic hypothesis of cancer", the overall hypothesis : Imaging mitochondria can assist in both the "prognostication" of freshly isolated tumors at the time of surgery, determine the potential of the tumor to response to metabolic modulators with acute studies in the explanted tumors as well as help with drug development strategies for metabolic modulators using cancer cell lines in vitro.

Thus this thesis consists of two parts, each addressing the two major objectives of this work. Part of the work presented in the second part, has contributed to the publication by Michelakis et al (2010) in Science Translational Medicine (*1*), on which I was a co-author.

Part A: Overview of Confocal Microscopy

A.1. What is Confocal microscopy?

Confocal microscopy is an imaging technique which allows the production of thin and sharp optical sections from thick tissue samples (*2*),(*3*). In conventional microscopy the light source illuminates the entire sample and light from above and below the focal plane of the objective contributes to the image (*3*). This out-of-focus light degrades the quality of the image by blurring it and limiting its resolution. Unlike standard white light or fluorescence microscopy, confocal microscopy excludes the out-of-focus light, allowing for the imaging of one thin plane (optical section) of the specimen at a time. A stack of these sharp optical sections can be reconstructed to form a full three-dimensional representation of the original specimen, similar to a CT scan.

Confocal microscopy can reconstruct images consisting of a number of fluorescence colors superimposed on the same field. By staining specimens (fixed or live) with

different fluorophores, different structures or antigens can be imaged simultaneously. The optical advantages of confocal imaging over conventional microscopy include reduced blurring of the image, improved resolution and signal to noise ratio as well as the ability to scan over a wide area and to clearly examine thick specimens. The electronic image processing capabilities allow for electronically adjustable magnification and contrast effects, the creation of 3-D reconstructions and quantitative measurements of optical properties of the specimen such as fluorescence or structure. The advantages over standard white light and epi-fluorescence microscopy make confocal microscopy particularly useful for investigating live cells and tissues. Confocal microscopy facilitates detailed functional imaging of processes in vivo or in vitro where fluorescence shifts can indicate changes in metabolic states. Imaging various fluorescence channels simultaneously allows diverse processes to be visualized concurrently so that their interrelationship may be explored. (*2*)

A.2. General Principles of Image Resolution

X Y Lateral Resolution:

The theoretical principles which underpin the foundations of modern light microscopy were set forth over a century ago in the 1870's by Ernst Abe. He showed how the angular image resolution was determined by the diffraction of light from the objective lens and the specimen. He determined the criteria required to design optics which were not limited by chromatic or spherical aberration and elucidated how the numerical apertures (NA) of the light condenser and objective determine the image resolution.(*3*) The NA is the range of angles (light cone) emanating from or converging on a point (P) over which an optical system can accept or emit light as the light ray travels from one medium to another (air to glass for example). It is defined as the product of the sine of the half angles (sin α) of the cone of light entering the objective or exiting the condenser multiplied by the refractive index (η) of the intervening medium. Figure 1 shows the simplified situation of a lens in air (η=1) (*3*).

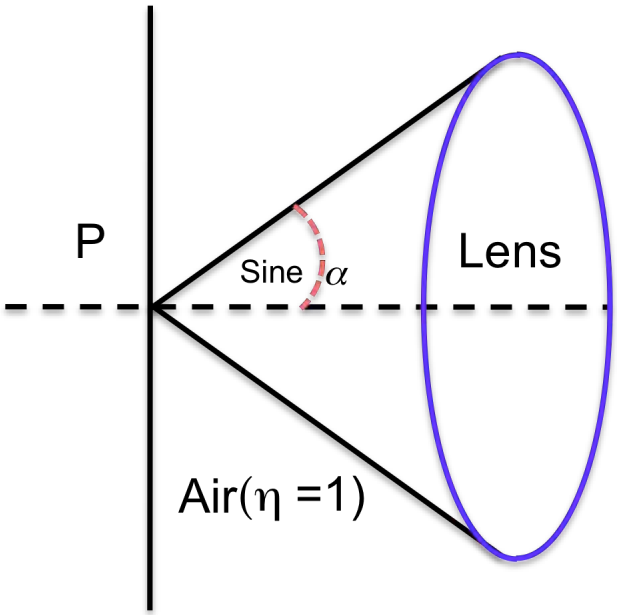

Figure 1: An illustration of the numerical aperture of a lens in air.

The numerical aperture can be used to calculate the minimum separation (d min) that two closely spaced lines can have and still be resolved as separate entities. The refractive index (η) of the medium (like air, water or oil) next to the objective or condenser must be taken into account when calculating their effective numerical aperture.

An image can also be thought of as being made up of light emanating from an infinite number of point objects. In reality, due to diffraction effects the image of an infinitely small point is not actually infinitely small but rather is seen as a circular image consisting of a central bright disk concentrically surrounded by progressively dimmer dark and light rings. This is called an Airy diffraction image. Two adjacent points in the image separated by a distance (d) have Airy disks which lie side by side and may overlap each other. As with the situation between two closely spaced lines, the minimum spacing that two adjacent points can have and still be resolved as separate entities can be determined. The radius rAiry of the first dark ring surrounding the central bright area can be calculated(*3*) from the numerical aperture NA**obj** of the objective and the light wavelength (λ*o*).

rAiry = 0.61 λ*o* / NAobj

When the distance (d) between two closely spaced points is greater than or equal to the radius of the Airy disk (rAiry) they are said to be resolved. This is called the Rayleigh criterion (*3*) and must be taken into practical consideration when adjusting the imaging parameters for maximum resolution . Thus the proper objective, immersion correcting fluids, mounting media, microscope slides and coverslips are very important for high quality imaging.

Z Axis Resolution:

The Z axis resolution is important for 3D imaging in confocal microscopy. It is the axial (up and down) three dimensional imaging resolution of the optical system. It is the minimum distance (Z min) that two points must be separated in an up and down axis and still be seen as separate entities. If we look at the 3D diffraction image of a point source around the focal plane we are examining a spherical region of light and dark patterns. For two closely spaced sources these light and dark patterns not only overlap horizontally but also vertically. Only light emanating from the region of the focal plane (the central cross section of the 3D diffraction pattern) is actually in focus but it is made up of a contribution from the overlapping diffraction images from above and below this plane. According to the Rayleigh criterion the resolution is determined by the minimum distance Zmin that two in-focus diffraction images (of the central cross section of the 3D diffraction rings) from two closely spaced points can approach each other and still be seen as separate entities (*3*). We can calculate the axial (up down) distance from the center of the 3D diffraction pattern to the first minimum (dark ring) if we know the numerical aperture of the objective (NA**obj**) , the refractive index of the medium between the object and the objective (η) and the imaging light wavelength in vacuum (λo)(*3*).

$$\mathbf{Z\ min} = 2\lambda o\,\eta\ /\ (\mathbf{NAobj})^2$$

Zmin is the distance that the microscope would have to be raised to focus the first intensity *minimum* of the 3D diffraction pattern onto the detector pinhole. As the NA**obj** becomes larger the axial resolution improves (Z min decreases) inversely proportionally with the square of the NAobj. The lateral resolution limit decreases only proportionally with the first power of the NA**obj.** This means that the minimum axial resolution Z min

of the objective improves faster than the lateral resolution rAiry as the NA of the objective increases. The ratio of the relative resolutions can be shown as:

$Z\ min / rAiry = 3.28\ \eta / NAobj$

Image Depth of Field:

In conventional light microscopy the contribution of light originating from above and below the focal plane of the image cannot be separated. Part of this contribution is sufficiently distant from the focal plane that it is blurry and indistinct. However part of this light is sufficiently close to the focal plane that it remains sharp and distinct. The distance above and below a single focal plane where light remains sharply focused is called the *depth of field*. The following points are important for the understanding and optimization of the *depth of field*:

1: The light that emanates from a single point is subject to geometric- and diffraction-limited spreading around the focal plane.

2: When directly viewed through the eyepiece, the optical irregularities of human eye itself affect the apparent depth of field. A properly designed optoelectronic detector system eliminates this problem.

3: The microscope's total magnification of the image is not a limiting factor if the magnification is large and the diffraction image of a single point (Airy disk radius) is much larger than the spacing and resolution of the detector elements.

Since 2 and 3 can be eliminated as limiting factors by proper design of the detector system, the actual depth of field (δ) can be approximated by

$\delta = 1/4(Zmin+ - Zmin-)$

Where Zmin+ is the distance of the first Airy minimum above the central Airy maximum, Zmin- is the distance of the first Airy minimum below the central Airy Maximum. So the depth of field δ is one quarter of the distance between the first Airy minimum above and below the central 3D Airy Maximum.

The contribution of the **diffracted** light (3D Airy pattern) from each point source above and below the focal plane is added to that of the **scattered** light from the out-of-focus areas. This out-of-focus light enters the objective reducing the contrast of the actual

image from the focal region. So for objects that are not extremely thin the out-of-focus light causes the apparent depth of field to be much larger than the actual axial resolution, resulting in degradation of the image quality. In conventional fluorescence or bright field microscopy there is no provision to exclude the out-of-focus light. This is the strength of confocal microscopy as it allows for the elimination of the unwanted light which expands the apparent depth of field. The light which is collected lies within the true axial resolution distance of the microscope optics resulting in a very shallow depth of field and extremely sharp image.

A.3 The development of Confocal Microscopy

The basic theory underlying the technique of confocal microscopy dates back to a 1957 patent by Harvard University postdoctoral fellow Marvin Minsky (*3*). His original patent consisted of a microscope using transmitted illumination, two identical objective lenses (one of which replaced the condenser of a conventional microscope), two pinholes and a stage scanning confocal optical system. (Fig 2).

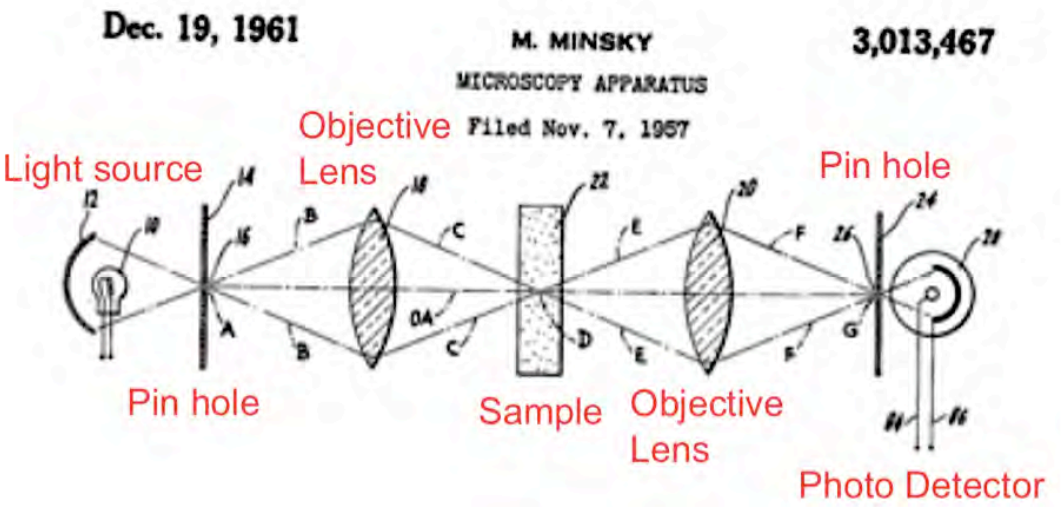

Figure 2: Schematic of the transmission confocal principle from Marvin Minsky's patent

This was then simplified using epi-illumination whereby a single objective served as both condenser and objective lens (*3*) (Fig. 3) This is the basis of current confocal microscope systems.

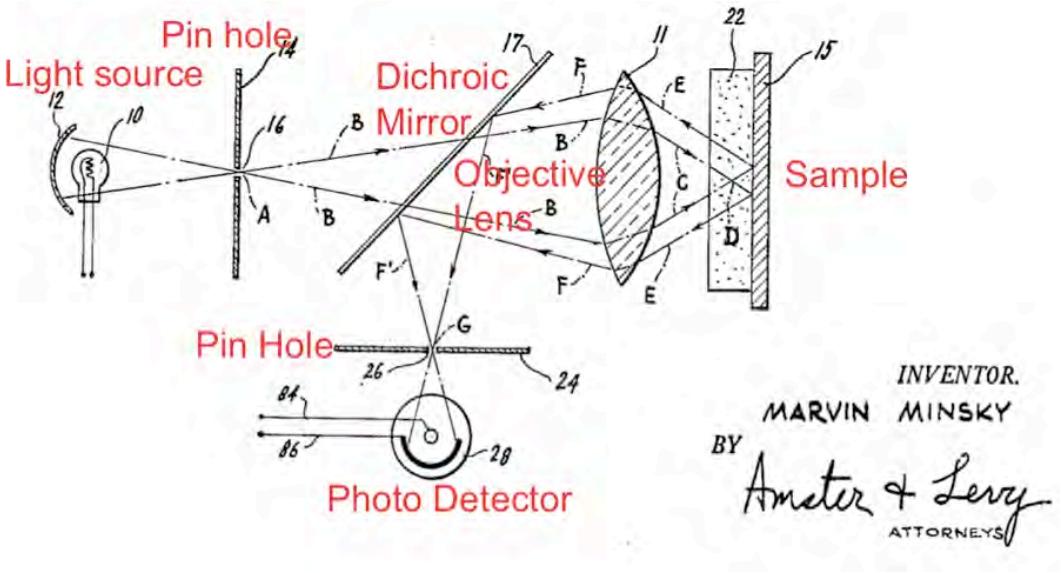

Figure 3: Schematic of the confocal epi-illumination principle from Marvin Minsky's Patent.

The light passed through the first pinhole as in Fig. 2, but then passed through a partially reflective or dichroic (transmits one wavelength but reflects another) mirror and entered the objective which focused a reduced image of the pinhole on the specimen. The light which was reflected off the specimen (not transmitted through it as before) passed through the same objective a second time striking the back side of the partially reflective or dichroic mirror. The light was then reflected out of the optical path by 90^{o} through the second pinhole into the photo detector.

Since only a small spot was illuminated at a time a full image was built up of sequential spots by scanning the stage back and forth in a raster pattern. The spot of light was detected by the photoelectric cell and the electrical signal produced was amplified and displayed on a long persistence cathode ray oscilloscope. The magnification was produced by the ratio between the scanning distance of the electron beam in the oscilloscope and the scanning distance of the spot of light on the specimen. This ratio which was variable resulted in very large magnifications. The disadvantage of this system was that because it required the whole microscope stage to be moved to scan the specimen, the image acquisition time was very slow. This was addressed with the development of the laser scanning confocal microscope(LSM) .

The LSM addressed the slow scan speed of the stage scanning microscope by scanning the laser beam rather than the entire mass of the specimen support stage. This allowed the entire specimen to be scanned very rapidly and thus corrected the problem of the slow image acquisition time.

Lasers as illumination sources :

The original design of early confocal microscopes used halogen, xenon or mercury vapour arc lamps for illumination. The development of the laser allowed for an alternative illumination source which corrected many of the deficiencies of these sources. The laser has the advantage of delivering a very high luminosity, highly collimated and tightly focused beam of a vary narrow range of wavelengths onto the target. Various types of lasers are now used for confocal microscopy. Commonly used are multi-line argon ion (458,488,514 nm), Helium Neon (HeNe) *medium* wavelength (543 nm) and Helium Neon (HeNe) *long* wavelength (633 nm) which are used to excite fluorophores ranging from green to deep red emission spectra. Widely used blue fluorophores such as DAPI (4',6-diamidino-2-phenylindole dihydrochloride) or the bisbenzimide dye Hoechst 33342 trihydrochloride trihydrate (390-465 nm bp emission filter) can be excited using a range of wavelengths. Commonly, Hoechst or Dapi are excited using a UV laser near its excitation maximum (around 350 nm) but the excitation spectrum of Hoechst or Dapi is quite wide allowing excitation (although much less efficiently) using a 405 nm laser as well. However, an infrared laser (outside of the excitation spectrum) may also be used to excite Hoechst or Dapi (and other fluorophores) in a process called multi-photon (or non-linear) excitation which I will describe later. These properties are important because these 2 fluorophores are typically used to identify the nuclei of cells and thus are used in the majority of images taken when studying cells and tissues.

Laser Scanning Confocal Microscope Development:

The modern laser scanning confocal microscope evolved in stages starting from developments dating back to the early 1970s. In 1972 Davidovits and Egger patented a laser illuminated confocal system where the objective lens was oscillated to scan the beam across the specimen. In 1977 Sheppard and Choudhury (*4*) published a detailed theoretical analysis of laser-scanning and confocal microscopy which laid the groundwork for subsequent developments. In the following years Sheppard and Wilson

described a stage scanning epi-illumination confocal system which used a laser source and a photomultiplier tube as the detector. This microscope was used for examining integrated circuits (ICs) and demonstrated that it was possible to reconstruct and display images over a much wider area than can be seen within the aperture of any objective lens in a conventional microscope and that if all the X-Y images made of the tilted surface of the IC during the Z slow scan were combined, an "extended focus" image of the whole surface could be produced. This showed that the depth of field of a confocal system could be increased or decreased with no loss of resolution (*3*).

The Modern Laser Scanning Confocal Microscope (LSM):

The previously described and other contributions from several groups ultimately resulted in the development of the modern type of laser scanning confocal microscope. The LSM in its current form was developed by Åslund et al. in 1983. This was followed by the publication of the biological applications of confocal microscopy by Carlson et al (1985), Amos et al. (1987) and White et al (1987). These publications set the stage for marketing of LSMs by companies such as Zeiss, Olympus, Leitz and Bio-Rad among others.

To illustrate an example of a modern LSM I will describe the Zeiss LSM 510 NLO (Non-Linear Optics) system with two photon capability. This is the system which was used to produce the images and data presented in part B of this thesis (Fig. 4). It consisted of the basic Zeiss LSM 510 NLO confocal microscope system with the addition to the imaging stage of a Warner RC-50/RLS sealed and temperature controlled heated imaging chamber (illustrated later) with flow through perfusion to allow imaging of living cells and tissues under close to physiologic conditions. Gases and pH could be monitored by sampling the chamber outflow and measuring the samples using a standard blood gas analyser.

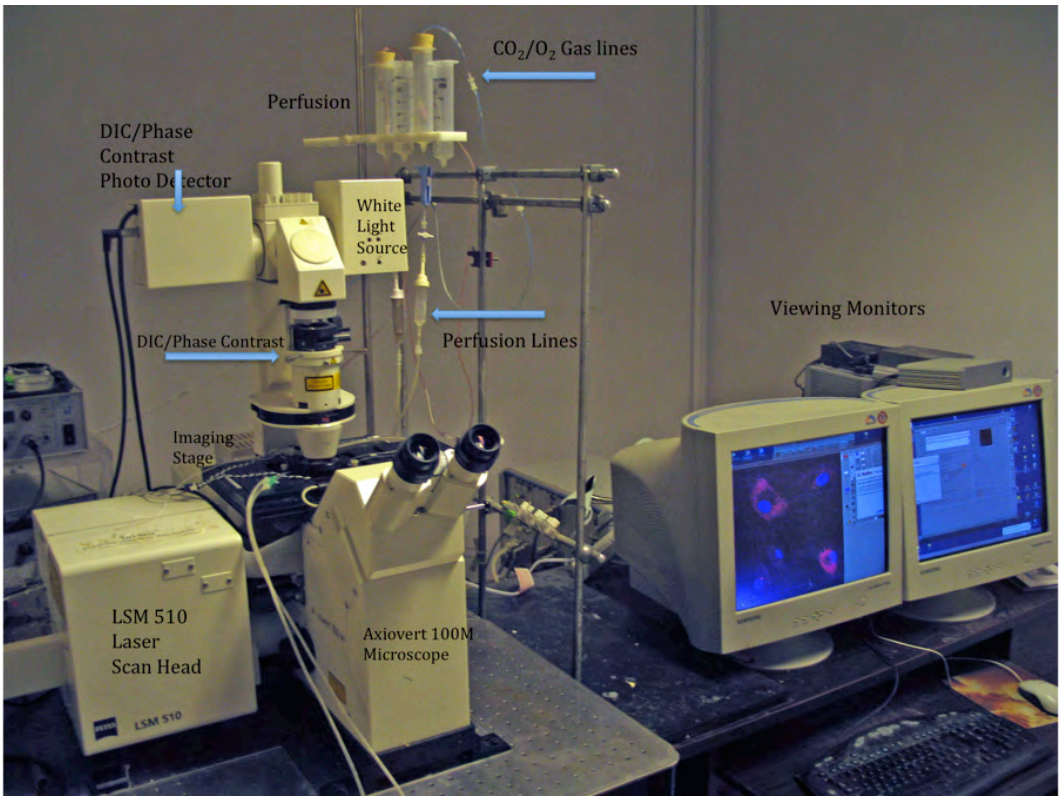

Figure 4: Zeiss LSM 510 Confocal Microscope with a perfused chamber

The modern LSM replaces slow and cumbersome stage scanning with the much faster laser beam scanning method. The various lasers employed replace the xenon and mercury arc lamps utilized in older systems. Unlike Minsky's original patent which used trans-illumination and two objectives, the much simpler epi-illumination with a single objective system is utilized.

The Zeiss LSM 510 NLO System:

The Zeiss LSM 510 NLO optical system in its basic form consists of a standard Zeiss Axiovert 100 M (or similar) inverted microscope stand with modifications to implement laser scanning confocal capability while still retaining normal non-confocal epi-fluorescence and bright field imaging capability. These modifications include the addition of an external scan head which has fiberoptic inputs to introduce the various laser beams into the optical path. Within the scan head there are adjustable collimators for each laser input which correct for the divergence of the beam exiting the optical fibre. Maintaining proper adjustment of these collimators is critical to assure maximum

delivery of beam power onto the target and the smallest focal spot size possible. After the collimators, a partially reflective mirror allows a small portion of the beam to pass through an attenuation filter to a monitor diode which indicates the laser input power. Most of the beam is transmitted to dichroic beam splitters which are reflective to one wavelength of light but are transmissive to a different wavelength. The dichroics reflect the laser excitation beam wavelength onto the scanning optics and then on through the objective lens onto the specimen. The wavelengths of emitted light return from the specimen back through the pinholes and the objective and onto the dichroics. The emitted light is now stokes shifted with respect to the excitation light and is transmitted through the dichroic rather than reflected. The light passes through the dichroics to the emission filters and into the photomultiplier tubes. The emission filters together with the dichroics select a narrow band of wavelengths emitted from the target and reject any excitation light which may be reflected from the target and any fluorescence wavelengths outside the range of interest. The scan optics consist of moveable galvanometer-mounted mirrors which cause the excitation beam to scan over the target in a **raster** pattern, that is traveling in a line from side to side starting at the top of the target and moving down one line at time to the bottom. The photons which ultimately form the image are detected by the photomultiplier tubes which produce an electrical signal corresponding to the strength of the light emitted from the specimen. This is amplified and reconstructed into an image by the imaging software of the associated computer to be displayed on a standard video monitor. The signal is simultaneously stored permanently in digital form for later image processing and analysis.

The microscope retains its conventional visual epi-fluorescence and bright field capabilities allowing direct visualization of the image through a standard eyepiece. The light source for direct visualization is not the lasers but rather a standard halogen or mercury arc lamp. The system is capable of recording both confocal and conventional photographic images because there are extra ports available on the microscope for the addition of extra cameras (either film or electronic) to directly acquire images independently of the computer system.

Beside the fluorescence image the system can also produce and record non-confocal transmitted light (grey scale) images using standard phase contrast (PhC) or differential

interference contrast (DIC) with either laser illumination for electronic image acquisition or white light (halogen) for direct visualization and photography.

Zeiss LSM 510 NLO (Non Linear Optics) Excitation Lasers:

The Zeiss LSM 510 NLO system's single photon excitation source lasers consist of a Lasos LGK 712ML4 (450-530 nm) Argon Ion multi-line laser, a Lasos LGK 7628-1 (633 nm) Helium Neon (He Ne) laser and a Lasos LGK 7786P (543 nm) HeNe laser. This system is also equipped with 2-photon imaging capability utilizing a Verdi V-5 532 nm (green) 5W diode pumped laser source which is wavelength multiplied and mode-locked by a Mira Model 900-F Titanium: Sapphire crystal laser. The output wavelength of the Mira is adjustable from 700-850 nm or 850-980 nm depending on the optical cavity installed. For our experiments the 700-850 nm cavity was used.

Multi-Photon Excitation Laser Scanning Microscopy:

Use of a laser near the excitation maximum allows a single photon (quantum) of light absorbed from the laser to produce one photon (quantum) of Stokes shifted emission from the fluorophore (*5*) (*6*). However, some fluorescence is emitted from the light cone above and below the focal point in a fairly linear relationship to the intensity of illumination in that area. This out-of-focus light would cause blurring and a general loss of image quality. To prevent this the light emitted from outside the focal plane must be excluded from reaching the photo detector. This requires that a pinhole be placed in the optical path to reject the out of focus light. Because the photons are absorbed along the entire path which they follow through the tissue, the depth and volume that can be imaged is limited to less than about 100 μm near the surface.

A second method of laser excitation which requires no pinhole, called multi-photon excitation (*6*) may also be used to produce fluorescence emission. This differs from single photon excitation in that a laser with approximately twice the wavelength of the single photon excitation source is used. This means that each excitation photon has only half the energy (quantum) required to produce fluorescent emission. Thus at least two photons (quanta) from the excitation source, each having half the quantum energy are required to be absorbed simultaneously by the fluorophore in order to produce one photon (quantum) of emitted light. Two photon excitation requires very specific conditions to function efficiently but has some major advantages over single photon

excitation. The laser beam must be of a very specific quality to operate in the two photon mode. The laser must be "mode locked" that is the vibrational modes of the laser cavity must be resonating with a fixed phase relationship. When the electromagnetic fields are in phase they add to each other producing a train of pulses emitted from the cavity. With proper design these pulses can be made to be of very short duration (femto seconds) and of extremely high intensity. Two photon excitation of the fluorophore only occurs when short duration pulses of sufficiently high intensity are absorbed. If the intensity is lower than the minimum threshold there is no two photon excitation and therefore no emission occurs. This threshold is only achieved at the small and intense focal point of the beam and therefore there is no emission from outside this area (Fig. 5).

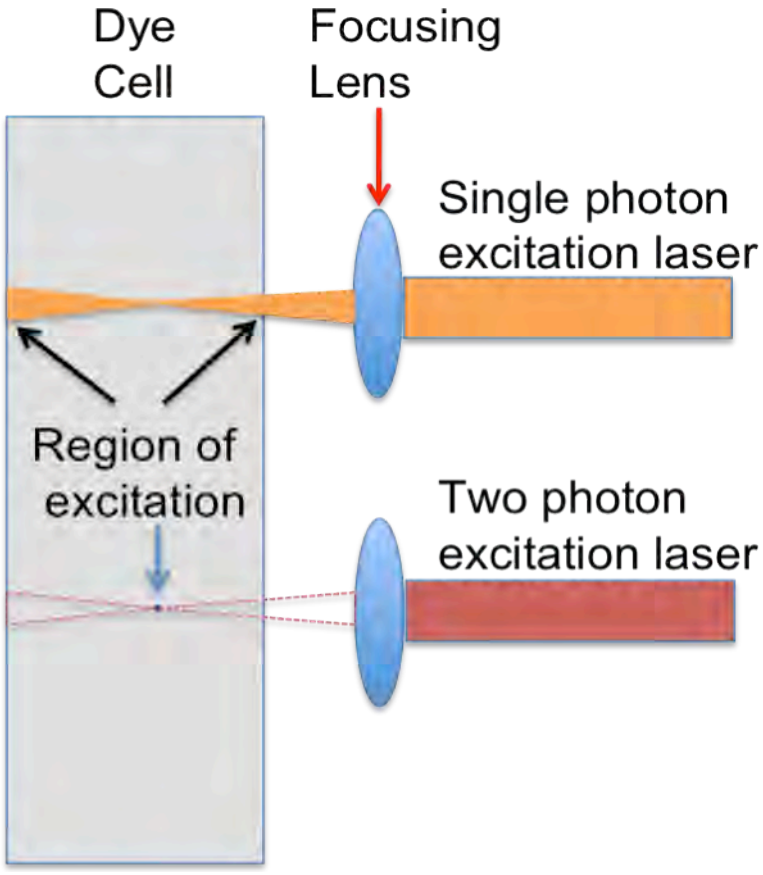

Figure 5: An illustration of single photon vs two photon excitation.
The black arrows indicate the region excited by single photon excitation. The blue arrow shows the small point fluorescing from two photon excitation.

This means that the fluorophore's emission comes from only this small focal point and since there is almost no out of focus light emitted from above and below this small

volume no pinhole is required as with single photon emission. Because the two photon laser used for confocal imaging is in the infrared range (700-850 nm) and has reduced absorption in the tissue compared to single photon sources, the damaging effects of the light (especially UV) like photo-toxicity and photo-bleaching, are minimized. This is a major advantage when live tissues or cells are imaged. Additionally, due to the reduced absorption, the longer wavelength infrared light penetrates deeper (up to 500 microns)(*5, 7*), into the sample than visible or UV light, allowing for a larger volume of tissue to be optically sectioned.

Three Photon Microscopy:

The advantages of two photon microscopy such as self focusing (improved optical sectioning), deep tissue penetration (a few hundred microns) and reduced photo-damage, can be further enhanced if an even longer wavelength is used for excitation. It has been demonstrated (*8*) that a wavelength of 1,200-1,300 nm shows extremely reduced attenuation (low absorption) in biological tissues allowing enhanced penetration (up to 1 mm)(*9*) and reduced photo-damage. However, with these longer wavelengths, three photon excitation is required to impart sufficient quantum energy to the fluorophore to produce fluorescence. This requirement, however, confers a further advantage to three photon over two photon excitation. Three photon excitation depends on the cube rather the square of the excitation intensity. This means that only an extremely small point at the focus has sufficient energy to produce fluorescence. This point is even smaller than that for two photon excitation and produces an even better a spatial resolution. Three photon imaging allows for submicron three dimensional resolution while providing better functional molecule specificity and laser intensity inputs ten times higher than two photon with no observable tissue damage. Along with this, another process intrinsic to the three photon process called third-harmonic generation occurs. Normally this is a very weak process but the higher intrinsic input power made possible by the longer wavelengths used, allows it to be useful. This process is sensitive to and enhanced at the interfaces between structures but is diminished in a uniform medium. This means that wherever there is a change in optical properties from one structure to another a high contrast image is produced of the interface between them but not of the uniform medium on either side of the interface. This property can be used to finely discriminate the exact position of cell or organelle membranes in a way which would otherwise not be possible (*10*).

A4. Challenges of Fluorescence and Functional Imaging

Fluorescence:

Fluorescence imaging is the cornerstone technique used in Functional Confocal Microscopy. It allows for the sensitive imaging of metabolic and structural changes in biological systems in real time and under physiological conditions without interfering with the processes being studied, as well as the sensitive imaging of samples which have been fixed for later analysis. When performing fluorescence microscopy (whether conventional or confocal) a knowledge of the theoretical principles of fluorescence is useful for understanding the practical considerations which affect image quality and the reliability and reproducibility of data.

Fluorescence is a quantum process whereby orbiting electrons within molecules are boosted from a stable low energy state into to an unstable higher energy state by absorbing some external excitation energy (from higher energy electrons or photons for example). The electrons can only remain in this unstable state for a limited period of time and will spontaneously return (either directly or in a series of jumps) to a lower energy level (ground state). In order to return to a lower energy level the excitation energy that was temporarily stored must be released.

This energy can be emitted as photons (fluorescence) or transferred directly to other electrons (FRET). In the case of photon excited fluorescence the emitted light is of lower energy (longer wavelength) than the absorbed excitation light. This change in wavelength between the excitation and emission wavelengths is called the Stokes Shift.
It takes a specific quantum of energy (photon) to boost an electron from one energy level to another. If this amount of energy is not available then the electron will not change energy levels and no fluorescence will occur. As the energy of the excitation deviates from the required quantum energy the absorption becomes less efficient and the amount of light emission decreases.

Most fluorophores have a fairly narrow absorption spectrum at which they are excited efficiently and a fairly narrow range of emission wavelengths. For example (Fig. 6) the fluorophore FITC (Fluorescein Isothiocyanate) has a peak excitation wavelength centered at 495 nm (blue) and it emits a spectrum of light centered around 519 nm (green). Typically lasers centered at 488 nm (argon ion) are used to excite FITC. At this

wavelength the excitation efficiency is about 90% of that at 495 nm. This is close enough to require only a modest increase in the intensity of the excitation energy.

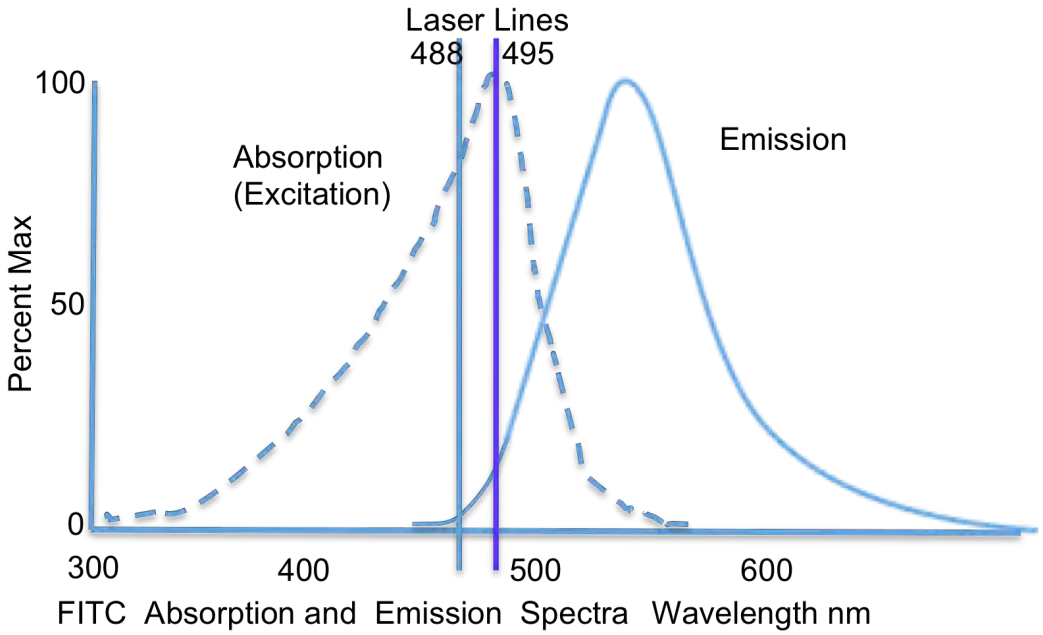

Figure 6: FITC absorption and emission spectra for 495 and 488 nm.

As one moves away from the characteristic absorption wavelength the excitation efficiency decreases fairly rapidly and the emission decreases correspondingly. However, if the excitation energy is applied at a high enough power it is possible to obtain emission even in the less efficient areas of the absorption spectrum. Typically lasers centered at 365 nm (UV) are used to excite Dapi or Hoechst. At this wavelength the peak excitation efficiency (100%) is produced (Fig. 7). But they can be excited at 405 nm (blue/violet) with a corresponding loss in efficiency (only about 10 % of the peak absorption). This requires a large increase in the intensity of the excitation energy. As one increases the excitation energy to very large levels, negative effects such as sample heating and fluorophore bleaching can occur. Therefore one wants to use excitation wavelengths that are as close as possible to the absorption peak.

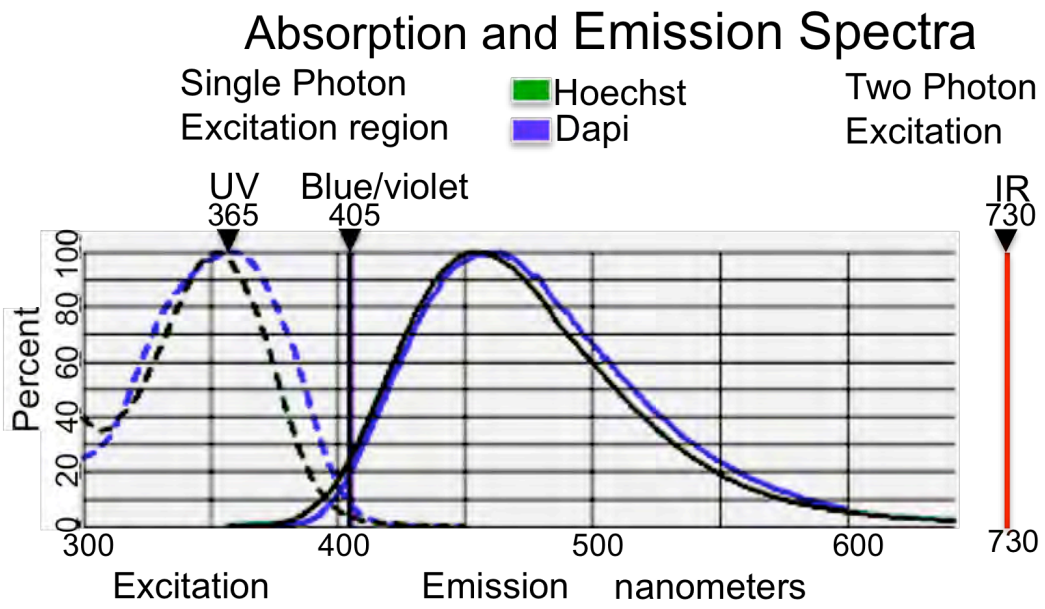

Figure 7: Single and two photon excitation and emission spectra for Dapi and Hoechst

Even though the excitation is most efficient around a certain wavelength, it is not necessarily the actual wavelength of the photon itself that is the limiting factor but rather the quantum energy that it imparts into the fluorophore. Fluorescence can be made to occur at excitation wavelengths far removed from the characteristics absorption spectrum if the correct amount of quantum energy can be delivered into the fluorophore (Fig. 6). Longer wavelengths equal lower quantum energy so if one photon of a long wavelength carries a specific quantum energy then a photon of half the wavelength will carry twice as much energy. For example if two long wave photons each carrying half the energy required for excitation can be absorbed by a fluorophore simultaneously then their additive energy is equal to one higher energy photon. The long wave photons need not be of identical wavelength or quantum energy, however, so long as their additive energy is sufficient to boost the electron to the required level to allow fluorescence. In order for this to occur the long wavelength excitation must be mode-locked to produce extremely short pulses (less than 100 femto seconds) resulting in high instantaneous power (10^2 to 10^5 W) (*11*). The probability of two photons being absorbed simultaneously is low and depends on the square of the instantaneous intensity. This is why the instantaneous power required for two photon excitation is so high. But to maintain average power levels at physiologically tolerable values the duty cycle (the on time versus off time) of the pulse train must be low. For example, a 100 fs pulse (100×10^{-15} sec) at a typical repetition

rate of 100 MHz (100 x 10^6 Hz) for Ti-Sapphire laser oscillators has an on time versus off time of only $1x10^{-9}$!

Autofluorescence:

One of the problems associated with fluorescence microscopy whether conventional or confocal centers around autofluorescence. This is the spontaneous emission of fluorescence from the sample when excited independently of the addition of any external fluorophores. This autofluorescence has a very broad spectrum which overlaps with most of the most common fluorophores. Some tissues and cells (like necrotic tissue, elastic lamina or erythrocytes) have autofluorescence which at times can be as strong as the desired fluorophores. Some of the main sources of autofluorescence in mammalian cells are endogenous fluorophores like the flavins and flavoproteins (FAD and FMN) which have the same excitation and emission profile as Fluorescein along with lipofuscin pigments and reduced pyridine nucleotides (NADH and NADPH) which can be excited by UV or two photon excitation(*12*). This causes an unwanted background (noise) signal which can interfere with or even mask the desired signal markedly decreasing the specificity of the signal. Tissues samples are especially prone to autofluorescence if improper fixation technique is used. Autofluorescence can be reduced by proper tissue preparation techniques and by intentional photobleaching or chemical treatment ($NaBH_4$) before staining. Autofluorescence can, however, have a practical application if it is desired to determine the presence of the very proteins and molecules (such as NADH and FAD) which spontaneously fluoresce when illuminated by the light source.

Photobleaching and Free radicals:

Another problem associated with fluorescence microscopy is photobleaching, whereby the desired fluorophore is degraded by the excitation wavelengths used to visualize the sample. This causes the fluorophore to gradually dim as it is exposed to light. The higher the laser the power and the longer the dwell time of light impinging on the sample, the greater the amount of photodamage and bleaching will be. This can be especially problematic if one is doing a 3D stack of a section of tissue and sweeps the same area continually until the required number of images are obtained. For example if 20 images are made at a fixed laser power each sweep would cause a reduction in signal. Depending

on the conditions the last image could be 50% or more dimmer than the first image. If quantitative analysis is done this could severely skew the results.

One way that bleaching might be caused is through unwanted multiphoton absorption. If the fluorophore in its normal excited state absorbs additional photons which boost it to an extra high energy state then bond dissociation could occur. The severity of bleaching seems to be dependent on the presence of molecular oxygen. Any oxygen present in the mounting compound will react with the triplet state of the excited dye and produce highly reactive singlet oxygen. The singlet oxygen produces free radicals which react with and bleach the adjacent fluorophores. This would continue until all the oxygen is used up and further bleaching would then cease. However if oxygen continues to diffuse into the sample, bleaching would continue at a level determined by the rate of O_2 replacement. The lifetimes of dyes can be significantly increased if O_2 is excluded from the sample. This however may not be practical so chemical antifading compounds have been developed. Antioxidants such as propyl gallate, hydroquinone and *p*-phenylenediamine can be added to the mounting compound of fixed specimens. These chemicals work by deoxygenation and through the quenching of dye triplet states and free radicals. Commercial preparations like Prolong Gold and Vecta Shield mounting compounds for use with fixed samples are available for this purpose. Obviously, the possibility of bleaching needs to be recognized and addressed in experiments where different levels of oxygen (for example hypoxia versus normoxia or hyperoxia) are used to determine the metabolic or redox responses of cells or tissues, particular when studying mitochondria biology.

Protecting live cells and preparations from photobleaching can be difficult. The previously mentioned compounds are unsuitable as they would be poisonous at the high concentrations required. Imaging under a low oxygen environment would be a possibility where it is appropriate for the samples involved but this has limited application. Fortunately, naturally occurring substances are available for this purpose. Singlet oxygen quenchers like carotenoids could be employed to protect the preparation. Some carotenoids like carotene itself are highly hydrophobic so a water soluble form must be used. Two interesting candidates are crocetin, the chromophore that colors saffron (*12*) and the synthetic aromatic retinoid etretinate, but unfortunately their endogenous fluorescence could interfere with the imaging of some fluorophores. Other possibilities

exist like ascorbate, histidine, cysteamine, imidazole, uric acid and some vitamin E analogues. All of these are water soluble, colorless and non-fluorescent. However they have low reaction rates and are consumed in their reaction with singlet oxygen requiring their use at relatively high concentrations.

The most effective way to reduce photobleaching is to work with as low a laser power as possible and for the shortest period of dwell time on the sample. Some preparations stained with certain fluorophores (like TMRM) will lose fluorescence when exposed to the epifluorescent UV light source used for initial focusing of a specimen. For functional imaging it is important to visualise biological specimens using only the Halogen (white light) source and for as short a period of time as possible.

Functional Imaging of Biological Processes:

Functional imaging is a dynamic process whereby live tissues, individual cells or organelles (e.g. mitochondria) are observed under controlled conditions, usually in real time, using various physiologic or metabolic indicators which can display functional changes in their metabolic, chemical or metabolically driven morphological state over time. Chemical metabolic changes that can be studied with confocal microscopy can include such processes as the opening and closing of ion channels, shifts of intracellular or intra-organelle calcium, glycolysis or glucose oxidation profiles, changes in the redox state of a cell, mitochondrial membrane potential, production of reactive oxygen species or changes associated with apoptosis.

As well one can use static imaging techniques to observe functional changes at a single "snapshot" in time by imaging cells or tissues that have been fixed after some intervention (such as a drug treatment) preserving some aspect of the metabolic state of the sample at that time.

The software of modern confocal microscopes allows for the automatic reuse of settings between imaging sessions. So all the adjustments to laser power, pinhole size, signal amplification along with contrast and brightness settings can be stored and automatically applied to the next imaging session. This allows for imaging under standard conditions between experiments and permits direct comparisons between images produced on different days or experimental conditions.

Conditions for Functional imaging of cells:

In order for functional imaging to be successful and meaningful, the tissues or cells must be maintained in a viable and optimal physiological state throughout the data acquisition process. This requires proper handling and maintenance of the tissues or cells under carefully controlled conditions from the time they are first acquired until imaging is complete and any sudden changes in these conditions must be stringently avoided.

Ideally the specimens under investigation should be kept under normal physiological conditions at all times. These conditions can be closely approximated in a standard laboratory incubator. Here, environmental parameters such as temperature, humidity, O_2 and CO_2 levels can be carefully regulated and controlled. The specimens also must be grown in a medium which compares closely to the nutrient, electrolyte osmotic, pH and growth factor balance found under in-vivo conditions. These conditions also need to be controlled on the microscope stage and various methods and apparatus (such as imaging chambers) are available for this purpose.

Temperature Control:

When working with mammalian or temperature sensitive cells a proper physiological temperature (e.g. 37º C) is required at all times for normal function. The exception to this is when a condition of lowered temperature is required to reduce the metabolic rate in order to maintain viability until optimal conditions for normal function can be restored. This could be necessary when tissue samples are first acquired during surgery and placed in ice cold saline for a short period of time to reduce their metabolic requirements and maintain a sort of "suspended animation" until the samples can be transferred to a more optimum environment.

A temperature of close to 37ºC is required to maintain the optimum function of most mammalian cells in that most enzymes and metabolic processes are optimized to proceed most efficiently at this temperature. Although gross morphological changes may not be immediately apparent if the temperature falls outside of the physiological range metabolic processes may be quickly affected. When examining mitochondria for example, this is extremely important as the speed of their metabolic processes are slowed down as temperature decreases. This could change the mitochondrial membrane potential ($\Delta\psi m$) leading to erroneous conclusions when utilizing a membrane potential

sensitive dye such as TMRM. In order to maintain the temperature of the sample on the microscope various types of stage and objective heaters are available from companies such as Warner Instruments and Zeiss which will keep the specimen at the appropriate temperature during the imaging process.

Humidity Control:

Maintaining the proper humidity surrounding cells and tissues is of vital importance since most biological specimens are mainly water and require that humidity levels remain sufficiently high to prevent drying out. Even a momentary drying of cells growing in a culture dish (e.g. when the growth medium is being changed) can destroy their viability. To prevent the drying of cells, incubators are kept at 100% relative humidity. Even if the cells do not dry completely, evaporation can cause concentration of the electrolytes in the growth medium changing its osmolarity and possibly killing or damaging the cells. This is especially important when using a stage heater on the microscope as evaporation can quickly cause loss of water from the specimen if no provision is made to maintain the proper humidity around it. Again companies such as Warner Instruments and Zeiss supply onstage imaging chambers which are sealed and maintain the optimum conditions around the sample.

Osmolarity , pH, Nutrients and Growth Factors:

These parameters are mostly controlled by the choice of growth medium and should closely approximate the optimum balance required for the vigour of the samples being studied. However, as previously stated humidity levels also can affect the concentration of components of the medium through evaporation. The pH of the medium can be affected by the ambient levels of O_2 and CO_2 but is usually controlled by the addition of a buffer such as bicarbonate, phosphate or TRIS. Ideally imaging on the microscope should be done using the same medium in which the cells were grown. Sometimes, however, interaction between components of the growth medium and the metabolic indicator with which the cells are stained makes this impractical (for example the interaction of media serum with AM ester conjugated indicators renders them impermeable to the cell membrane). This necessitates a modification of the imaging medium either by leaving out a certain component (e.g. serum free medium) or imaging in a solution such as KREBS or Hanks Balanced Salt Solution (HBSS) which at least maintain a buffered solution of the correct osmolarity. Although these solutions are not

adequate to maintain growth or proliferation they at least maintain adequate physiological conditions for the short duration of time required for imaging.

O_2 and CO_2 Concentration:

During the course of normal aerobic cell metabolism oxygen is consumed and carbon dioxide is excreted. Maintaining the proper concentration of gases is vital for maintaining viability and health of the samples being studied. As stated previously the concentrations of gases can affect other parameters such as pH. Carbon dioxide especially, has a strong effect on pH causing acidification (carbonic acid) of the medium but oxygen levels also have an affect. Any deviation of pH from the optimum value (7.35-7.45) is best controlled by maintaining the proper concentration of gases. However, some experiments require gas concentrations outside the normal physiologic values such as when investigating the effects of hypoxia. Hypoxia will cause changes in the pH value, this can be counteracted by the addition of extra buffer to the medium. This means that one has to be alert to this possibility and frequently monitor the pH and gas conditions by testing samples in standard blood gas analysis machines. Deviations from this practice not only affect the accuracy of the measurements but are frequent sources of "conflicts" in the published literature. That is, for example, identical experiments which produce opposite results due to a factor (such as a difference in pH) which varies between the two experiments and is not recognized and adequately controlled.

Imaging Chambers:

Imaging chambers are available which can be placed on the stage of a microscope and act as a sort of mini incubator. If so equipped they can maintain the sample at physiologic temperature, humidity, nutrients and under the desired mix and concentration of gases. The specimen is placed in the chamber over an imaging window which is positioned above the objective of the microscope. The top of the chamber is closed over the sample sealing it off from the ambient conditions. When using a heated sealed chamber to maintain proper temperature and humidity the O_2 and CO_2 levels can quickly stray outside of physiological values and the nutrients in the imaging medium may become depleted. This is especially vital to control when dealing with whole tissue samples because due to the mass of biological material present the metabolic requirements may be quite high and the levels of gases, waste products and nutrients may quickly become unbalanced. Needless to say this could severely compromise the

integrity of the data obtained. These problems can be addressed by perfusion of the chamber using a buffered solution which has the proper concentration of gases and any required nutrients dissolved in it. By flowing this solution through the chamber, metabolic waste products (e.g. lactic acid) are constantly removed and normal physiologic conditions are maintained. Occasionally, custom-made modifications of commercially available chambers are required.

An example from Warner Instruments is shown in Fig. 8.

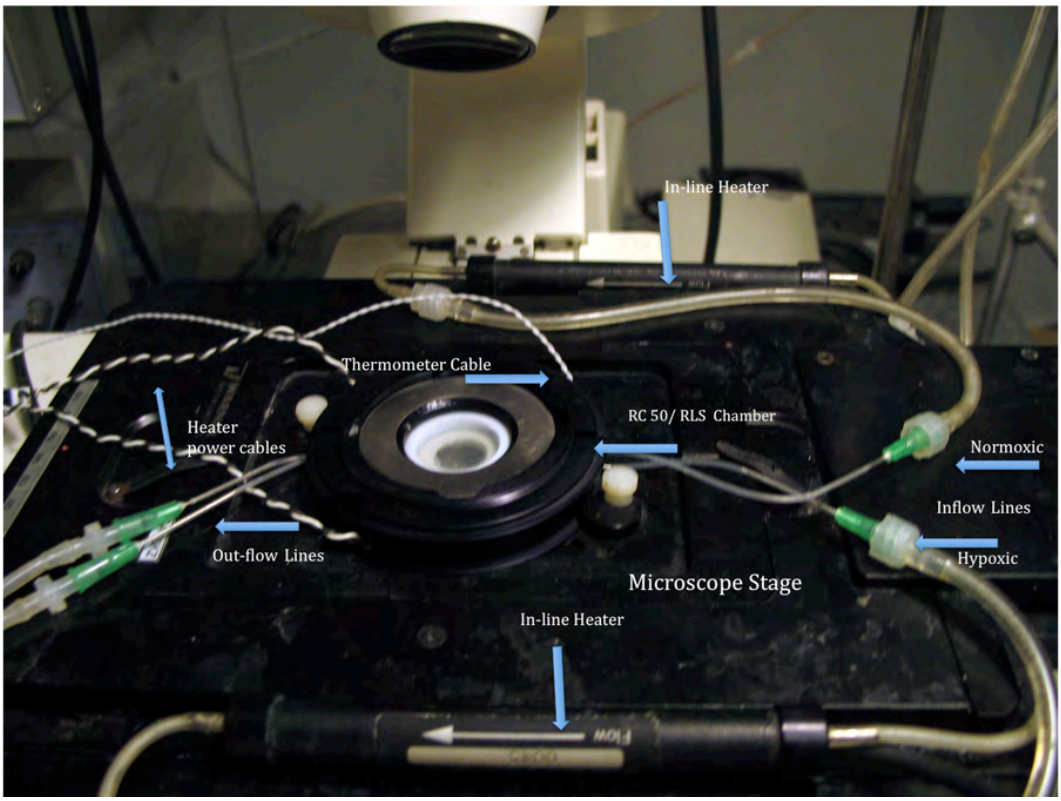

Figure 8: Warner RC-50/RLS heated and perfused sealed imaging chamber

Practical Considerations for Functional Imaging:

Since cells and tissues must be kept in aqueous media to remain viable, the choice of coverslip, objective and refractive index (η) of the correction fluid is important to produce the brightest and best quality image. So for example at 546 nm an aqueous medium has a (η)=1.33, air (η)=1, plastic (η)=1.34, glass (η)=1.518 and an immersion oil like Zeiss Immersol$_{TM}$ has a (η)=1.5180. When visible light rays pass from one medium to another of a different refractive index (η) (ex. water (η)=1.33 to air (η)=1 to glass coverslip (η) ~1.518, the path of the light rays is bent (refracted) resulting in defocusing, distortion and loss of resolution. As well, a certain amount of light is

reflected back at each interface resulting in loss of brightness. These effects become more pronounced as the difference in refractive index between the two media becomes greater and also change with temperature and the light wavelength. For example the refractive index of Zeiss Immersol$_{TM}$ changes from 1.5307 at λ=435.8 nm to 1.5098 at λ=589.3 nm. When imaging samples in aqueous media (η)=1.33 these effects can be minimized by choosing an objective designed for water immersion with water as the correction fluid (η)=1.33 and a coverslip made of a material which matches the refractive index of the medium and correction fluid as closely as possible. In this case a plastic coverslip or CYTOP$_{TM}$ fluoropolymer (η)=1.34 would be superior to glass. The thickness of the coverslip is also important and will often be specified for the particular objective. Note that oil immersion objectives (η=1.518) have a refractive index which is very different from aqueous media and will give a poorer image quality when used to image "wet" live specimens. Oil (and glycerine(η)~1.473) objectives are best used for fixed specimens mounted in a compound which has a refractive index closer to these (η~1.45-1.55). Some objectives like the Zeiss LCI Plan Neofluar 25 X objective have an adjustment collar which allows them to be set for water, glycerine or oil to match different imaging conditions. It is very important to carefully match the sample, objective and correction fluid as the differences in image quality can be very large, especially at high magnifications.

Image Processing:

The digital images produced may be further processed and manipulated by imaging software. For 3D imaging, deconvolution software can apply a mathematical algorithm to the digitally stored data, deblurring the image to improve displayed image quality. The enhancement of sharpness and contrast facilitates quantification and analysis of acquired data. The software can measure brightness, contrast, chroma values, etc. down to the level of individual pixels. For example when quantifying apoptosis using the technique of TUNEL staining, the contrast of the image can be enhanced to sharply define the TUNEL positive green nuclei to facilitate the counting process. This counting can be done visually but this is very time consuming. Generally a program such as Image Pro plus can be used to automatically and very quickly enumerate the TUNEL-positive cells. In the same way the image processing software can be used to choose "regions of interest" (ROI) by drawing around the area with the cursor and enclosing a defined zone for which the relative brightness of the different fluorophores can be simultaneously measured and

quantified automatically. This is used for such imaging as measuring mitochondrial membrane potential with the potentiometric dye TMRM. For example, the brightness of the TMRM (red) signal in untreated cancer cells can be compared to the brightness in cancer cells treated with a drug and the relative difference in membrane potential can be directly quantified to assess the effect of the drug.

Part B. Functional Mitochondrial and Metabolic Imaging

In this section I first summarize essential concepts of cellular and cancer cell metabolism and mitochondrial function. Then I list the methodology used with an emphasis of practical considerations and troubleshooting. Finally I present a series of experiments to support the idea that confocal microscopy can be used as a tool to determine the aggressiveness of tumors at the time of tumor surgery, their potential to respond to metabolic modulators as well as to guide drug development programs in vitro.

B1. Background

Evolution of metabolism and mitochondria:

The first life to evolve on earth developed under environmental conditions devoid of free oxygen. These organisms developed an anaerobic metabolism which was capable of supplying the cells' energy needs without the need for oxygen. This process would have been the precursor of the glycolytic pathways that are still found in modern anaerobic organisms and as the first step in the energy production pathway of aerobic organisms. With the appearance of cells capable of photosynthesis, conditions on the early earth began to change. Oxygen as a by-product of photosynthesis began to accumulate in the atmosphere of the early earth. This increasing oxygen concentration posed a metabolic challenge since it was chemically damaging (oxidizing) and thus a potent poison. In order to survive these changing conditions organisms were required to either retreat into any anaerobic niche they could find or to evolve biological strategies to counteract the deleterious effects of oxygen gas. Organisms thus developed enzymes capable of scavenging and detoxifying the free radicals produced by oxygen's effects within the cell. This challenge actually proved to have been an opportunity for one group of organisms which developed a way to not only counteract the damaging affects of O_2 but also to utilize it to develop a novel energy production strategy that made use of its oxidative properties. The old process of glycolysis was not particularly efficient in that it made available only a fraction of the chemical energy that was contained in the nutrients

that organisms consumed. These new organisms developed a way to break down the nutrients in a step wise manner releasing some energy (electrons) at each step. By reacting oxygen with the nutrient molecules, high energy electrons became available to produce the energy transferring molecule adenosine triphosphate (ATP) used for the metabolic processes of the cell by a process called chemiosmotic coupling. It is now thought that at some point early in the history of life one group of these organisms, as free living prokaryotic (having no defined nucleus) bacteria, physically entered into another group of early glycolytic eukaryotic (cells with a defined nucleus) organisms lacking the ability of chemiosmotic coupling. As it turned out the products of glycolysis were extremely suitable for the chemiosmotic bacteria to use for the first step of their energy production pathway. This resulted in a symbiotic relationship between the two whereby the host transferred the products of glycolysis as metabolic substrates to the symbionts and received the products of enhanced energy efficiency in return. This symbiosis became so entrenched that the engulfed bacteria (the precursors of mitochondria) actually transferred most of their genome into the host cells' nuclei. So like a virus they forced the host cell to replicate more copies of themselves by inserting their own genome into that of the host. Once they became dependent on their host cells for reproduction they permanently lost the ability to exist as free living organisms but assured their continued existence as permanent (and vital) organelles within the cell as mitochondria. Mitochondria are found within virtually all modern eukaryotic organisms and are the energy powerhouses of the cell. However, although mitochondria are responsible for providing most of the energy required to keep a cell alive they can also bring death upon the cell through the process of apoptosis (controlled cell death). The metabolic and apoptotic pathways converge in mitochondria which are dependent on the cell for their own continued existence but are still able to exercise some control over the life and death of the cell. This is especially important if a cell is damaged genetically and therefore potentially dangerous to the organism.

Mitochondrial Structure:

The mitochondrion (*13*) has a plasticity in its shape ranging from an elongated cylindrical (wormlike) shape to round in shape and can vary in diameter between 0.5 to 1.0 μm in eukaryotic cells. It is usually found associated with other mitochondria and the endoplasmic reticulum but is quite mobile fusing with other mitochondria to form chains and then separating again. The mitochondrion consists of two specialized membranes

and two internal compartments. The outer membrane is separated from the inner membrane by a narrow intermembrane space which constitutes one of the internal compartments and can be considered to be equivalent to the cytosol of a cell. The inner membrane defines the other internal compartment the mitochondrial matrix. The outer membrane is permeable to molecules of 5000 Daltons or less through the many large aqueous channels formed by transport molecules called porins which span the lipid bilayer. Molecules may pass through the outer membrane to the intermembrane space with relative ease but most cannot pass through the inner membrane to the matrix because of its impermeability. Most of the biochemical functions of the mitochondria occur in the matrix and the inner membrane. Only selected molecules which are required to participate in these reactions are actively transported from the intermembrane space into the matrix. The inner membrane is made up of a large proportion of the phospholipid cardiolipin which contains four fatty acids in its structure rather than two, the result of which is that the membrane is made highly impermeable to ions. To facilitate the import into the matrix of those small molecules required for the functioning of the mitochondria a number of highly selective transport proteins are found in the inner membrane. To allow for more efficient transfer of the required small molecules the surface area of the inner membrane is greatly increased by highly convoluted infoldings called cristae which vary in number according to cell type (Fig. 9). Cells with higher metabolic needs have more cristae in their mitochondria than those with lower metabolic requirements. The enzymes which metabolize pyruvate and fatty acids to produce acetyl CoA and those which oxidize it in the citric acid pathway are found in the matrix. The enzymes of the electron transport chain (respiratory chain) are embedded in the inner membrane and this is were oxidative phosphorylation by ATP synthase (a molecule of about 500,000 Daltons) produces most of the ATP required for metabolism.

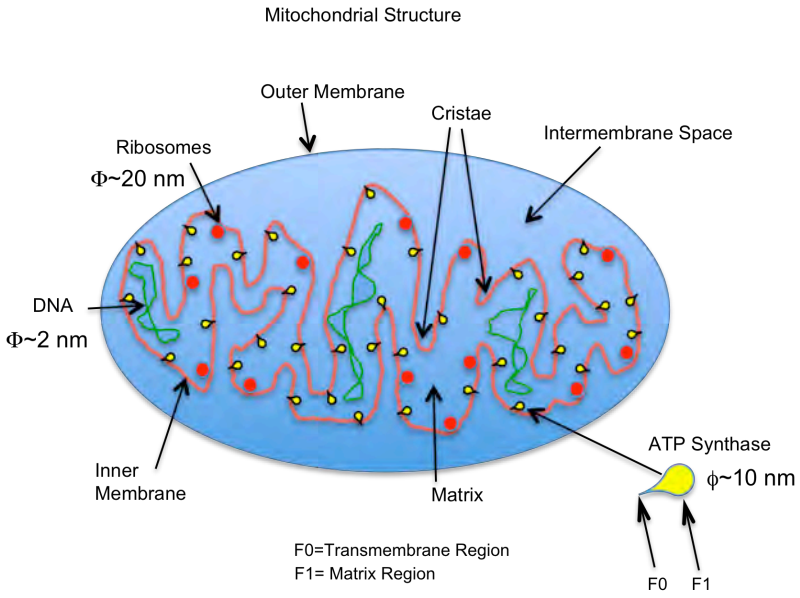

Figure 9: The compartmentalized structure of the mitochondrion

Apoptosis and the Mitochondrion:

There are two main apoptotic pathways in the cell, the mitochondrial (intrinsic) pathway and external receptor mediated pathway (extrinsic). At any given time the apoptotic versus anti-apoptotic signalling determines whether a cell will be allowed to divide and proliferate, remain quiescent or die and thus mitochondria are critical regulators of the cell's homeostasis. Cells that display abnormally suppressed apoptosis may (like cancer) multiply out of control while cells that display abnormally increased apoptosis may be found in a degenerative disease like Alzheimer's. The proteins of the intrinsic pathway can be affected by oncogenes, being either up or down regulated for the benefit of the cancer cell rather than for the good of the host organism.

There is evidence that the mechanism of intrinsic apoptosis involves the regulation (either by suppression or enhancement) of pore formation within the mitochondrial membrane (*14*) (*15*) i.e. the mitochondrial permeability transition pore (MPTP). When this pore is opened, pro-apoptotic factors like cytochrome c or apoptosis-inducing factor, are released from the mitochondrial intermembrane space into the cytoplasm of the cell, initiating protein degradation and apoptosis.

ATP Production:

ATP is the primary energy currency of a cell. The metabolic processes in cells ultimately depend on the transfer of electrons mediated by ATP. Most of the cells within the human body produce the majority of their energy requirements (ATP) through the efficient process of oxidative phosphorylation (OP) which occurs within the electron transport chain of the mitochondria. Cancer cells on the other hand use the less efficient process of aerobic glycolysis in the cytoplasm for ATP production and bypass the process of oxidative phosphorylation. (*16-19*) This is known as the Warburg effect.

The production of energy (ATP) within the cell is a multistep process consisting of three distinct but ultimately interrelated pathways.

1: Glycolysis (aerobic and anaerobic), i.e. the Embden-Meyerhof Pathway

2: Krebs' Cycle (Citric Acid Cycle or Tricarboxylic Acid Cycle)

3: Oxidation through the electron transport chain (Oxidative Phosphorylation).

Under aerobic conditions in non-cancer cells glucose oxidation (GO) and fatty acid oxidation (FO) produce most of a cell's ATP by oxidative phosphorylation (OP) (*20*). Which process is more important depends on the cell type. Amino acids can also make a contribution (*21*) if the other fuels are in short supply (under conditions of starvation for example). But since the main difference between cancer cells and normal cells is how they obtain their energy from glucose, for the purposes of this thesis I will concentrate on the process of glucose oxidation.

Briefly, the main steps involved in ATP production from glycolysis to glucose oxidation (oxidative phosphorylation) can be described as follows:

Monosaccharide (hexose) sugars derived from the food intake of the organism (disaccharides are hydrolysed to monosaccharides in the intestine) are transported into the cytoplasm of the cell where the first step required in the processes of both aerobic and anaerobic glycolysis occurs. The sugars are converted into an intermediate form which makes them suitable to enter into the glycolytic pathway. Glycolysis then proceeds with the net production of 2 ATP and 2 pyruvate molecules per sugar molecule. In aerobic conditions pyruvate is transported into the mitochondria for further oxidation and is converted into acetyl-CoA, which enters the Krebs's cycle. Through the Krebs' cycle, electrons (in the form of NADH and $FADH_2$) are donated to the ETC complexes down a

redox gradient. For every electron donated, a hydrogen molecule (positively charged) leaves the inner mitochondrial membrane. This creates a very negative membrane potential of more than -220mV (the mitochondria are the most negatively charged organelles of the cell). This membrane potential is used at the last part of the ETC (i.e. complex 5) where this stored energy is used to support the phosphorylation reaction required to make ATP. Overall, every molecule of Glucose that is oxidized in the mitochondria, yields ~36 molecules of ATP, i.e. this is 18 times more efficient a process for energy production compared to the cytoplasmic glycolysis.

The fact that the degree of the mitochondrial potential (i.e. $\Delta\Psi m$) is linked to the energy production process suggests that it can be used as an index of mitochondrial function. Importantly, the opening of the MPTP is voltage dependent. The more negative the $\Delta\Psi m$ the higher the threshold for MPTP opening and in contrast, the lower the $\Delta\Psi m$ the easier for the MPTP to open. **Thus the $\Delta\Psi m$ is an index of both mitochondrial function and resistance to apoptosis.** For example, almost all solid tumors and cancer cells have very high $\Delta\Psi m$ compatible with their very high resistance to apoptosis and drugs that can reverse this mitochondrial hyperpolarization may facilitate cancer apoptosis. This is further discussed below.

Cancer cell Metabolism:

Normal cells produce most of their energy requirements (ATP) from glucose by the efficient process of GO but cancer cells maintain a glycolytic phenotype producing most of their energy needs by the inefficient process of glycolysis this is called the Warburg effect after it discoverer Otto Warburg.(*18*)

Respiration is coupled to oxidative phosphorylation so $\Delta\psi m$ is an index of activity of mitochondria. The higher the $\Delta\psi m$ (hyperpolarization) the less GO is occurring in the mitochondria and more glycolysis is required to meet the energy needs (ATP production) of the cell. Cancer cells are characterized by greatly increased $\Delta\psi m$ indicating a suppression of GO and reliance on glycolysis to meet their energy requirements. Since most cancers are characterized by aerobic glycolysis not GO (*22*) they have greatly increased glucose uptake because as previously described glycolysis is far less efficient at producing ATP than oxidative phosphorylation (glucose oxidation). This upregulated glucose uptake is the basis for the PET FDG technique (measurement of fluoro-deoxy-

glucose uptake using Positron emission Tomography), which remains the most sensitive technique to diagnose cancer. This is because this extreme glycolytic shift even n the presence of normoxia is a unique feature of cancer, distinguishing it from the surrounding healthy tissues. Thus, targeting this metabolic switch may be a selective means of treating cancer.

The advantages of using glycolysis instead of GO in cancer cells:

When tumors first begin to grow they are poorly vascularised and start developing under a state of poor oxygenation (hypoxia). Hypoxic conditions activate hypoxia inducible factor (HIF). Hypoxia inducible factor (HIF) activates many enzymes of glycolysis as well as upregulates glucose transporters (*23-26*). The activation of the HIF pathway also promotes activation of angiogenesis. This causes tumors to enter a glycolytic state while at the same time becoming more highly vascularised by the HIF pathway. But the glycolytic profile persists even with sufficient vascularisation and oxygenation. This aerobic glycolysis with suppressed GO requires cancer to utilize large amounts of glucose to meet its energy (ATP) needs. Cancer uses glucose transporters to increase glucose transfer into cells and these glucose transporters are upregulated by HIF. This glucose is converted to pyruvate by the enzymes of glycolysis. Normally this pyruvate would be transported to the mitochondria and converted to acetyl Co-A by pyruvate dehydrogenase (PDH). But the enzyme pyruvate dehydrogenase kinase (PDK) is upregulated in cancer by HIF as well. PDK phosphorylates and so inactivates PDH preventing it from converting pyruvate to acetyl Co-A. The pyruvate accumulates in the cytoplasm where it is then further broken down into lactic acid. This lactic acid builds up leading to a state of lactic acidosis. Increased lactic acid in lactic acidosis facilitates tumour growth by the breakdown of extracellular matrix allowing expansion by increased cell mobility (metastatic potential). In addition, pyruvate and other glycolytic intermediates, can also be shifted toward other anabolic pathways that are important in highly proliferative cells, including amino acid and lipid biosynthesis. Recent evidence suggests that transformation to a glycolytic phonotype confers resistance to apoptosis as well (*19, 27-30*). For example, several glycolytic enzymes, have dual functions and are also important inhibitors of apoptosis. Therefore, the suppression of mitochondrial function in cancer offers several proliferative advantages including inhibition of apoptosis and shifting of metabolites toward biosynthetic pathways critical for cancer cell proliferation. Thus reversing this metabolic switch could be a potentially *effective* cancer

therapy. Because this switch to glycolysis is a critical difference between cancer and most healthy tissues, it may also offer a *selective* therapeutic target (*25, 31-33*). By promoting GO and reversing the glycolytic metabolism in cancer, metabolic modulator drugs like dichloroacetate (DCA) can inhibit tumor growth.

DCA Mechanism:

Dichloracetate (DCA) is a small 150 Dalton molecule that can penetrate all tissues, even traditional chemotherapy sanctuary sites like the brain. DCA activates pyruvate dehydrogenase (PDH) by inhibiting PDH kinase (PDK) at a concentration of 10-250μM in a dose-dependent fashion (*34*). There are four PDK isoforms that are constitutively expressed in most tissues with the most sensitive to DCA being PDKII (*35*). The crystal structure of PDKII bound with DCA is shown in Fig. 10, where the carboxylate group of DCA forms a salt bridge with Arg-154 and the chlorine molecules reside in a hydrophobic pocket (*36*).

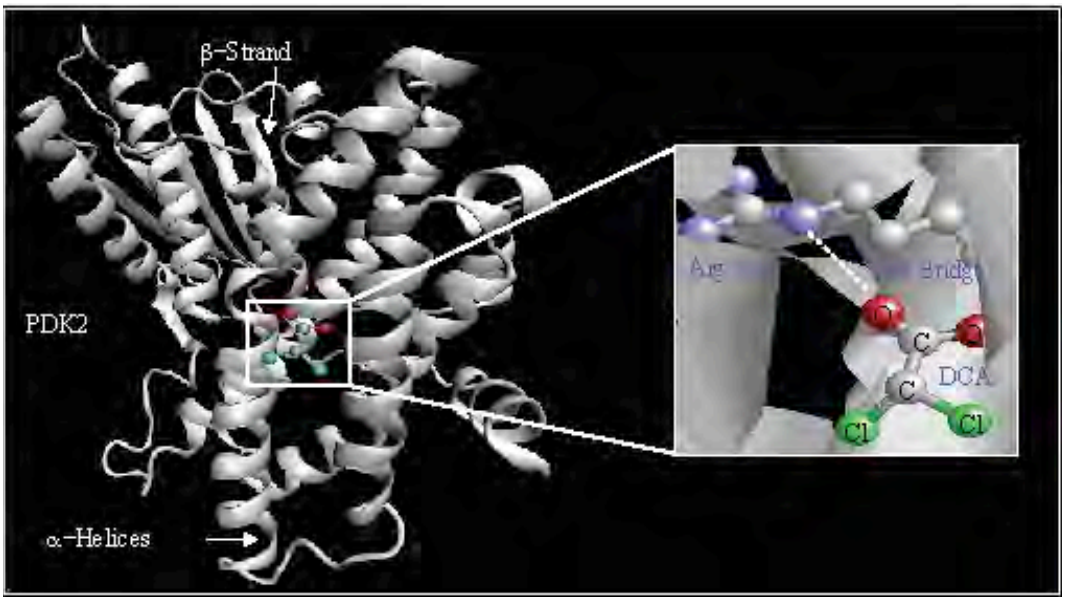

Figure 10: The molecular mechanism of PDK inhibition by DCA

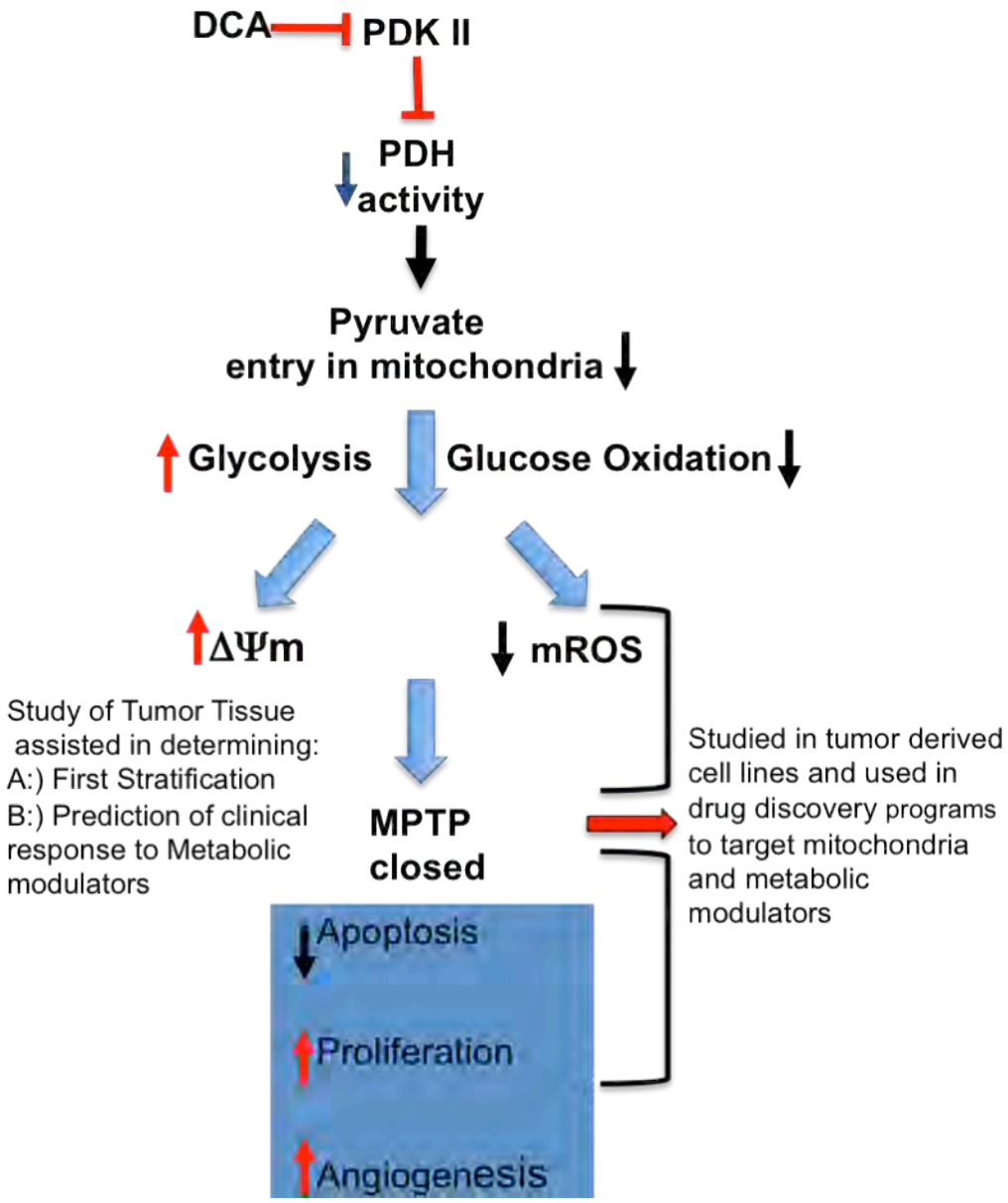

Figure 11: DCA action mechanism pathway.
PDKII increases glycolysis and Δψm, reduces mROS, reduces apoptosis and increases proliferation and vascularization . DCA blocks these effects by inhibiting PDK II.

DCA activates PDH, promoting the influx of pyruvate into the mitochondria, resulting in an increase in the GO to Gly ratio (*37*). This is associated with reversal of mitochondrial hyperpolarization, an increase in mitochondrial reactive-oxygen species (mROS) and activation of mitochondria-dependent apoptosis (*37*) (Fig.11)(*1*). The effects of DCA are mimicked by PDKII siRNA and there is no additional effect of DCA beyond PDKII siRNA, suggesting that the mechanism of action is PDKII inhibition (*37*). DCA

decreased tumor growth in several xenotranslant models including non-small cell lung cancer, breast cancer and glioblastoma (*37-43*). In a small but mechanistic clinical trial, oral DCA therapy in patients with advanced glioblastoma had similar effects on tumor mitochondria compared to the previously published animal and in-vitro studies (tissues taken before and after treatment), whereas DCA had no effects on healthy brain tissues taken from epilepsy surgery (*1*).

DCA was used in the experiments presented in this thesis as an example of a metabolic modulator that can be applied acutely in freshly isolated tumors or more chronically in tumor-derived cell lines to determine whether the cancer mitochondria would respond to PDK inhibition by increasing their mitochondrial function, evidenced by a decrease in mitochondrial membrane potential and an increase in mitochondria-derived reactive oxygen species (mROS). Such effects can be used to predict whether the patient from whom the tumor was removed, would also respond clinically to the chronic use of oral DCA therapy. This may be used as a biomarker in order to enroll in DCA clincial trials the patients with the highest likelyhood of responding to DCA and avoiding the delay in other treatment for patients that have a low likelihood of responding.

B2. Materials and Methods

The cell lines investigated were derived from

a) Primary cancer compared with metastasis from same patient

1. Primary Melanoma CRL 7425 and melanoma from Lymph node Metastasis CRL 7426
2. Colorectal Adenocarcinoma CCL228 and colorectal carcinoma from Metastatic Lymph node CCL 227

b) Primary cancer compared to non-cancer cells from the same patient

1. Mammary Ductal Adenocarcinoma HTB 126 and Mammary Gland Fibroblasts HTB 125
2. Lung Adenocarcinoma CRL 5868 and Peripheral Lymphocytes CRL 5957

c) Normal epithelial cell lines like Small Airway Epithelial cells SAEC CC 2547

d) Brain Tumor (Glioblastoma obtained at the time of initial tumor debulking surgery) and "Normal" noncancerous brain tissue obtained from epilepsy surgery.

All cultured cell lines were obtained from ATCC. Tissues were obtained from the Walter Mackenzie Health Sciences Center (University of Alberta Hospital) with the permission of our institution human ethics committee.

Cell culture:

All cells were grown in culture media appropriate to the cell line as obtained from the protocol supplied with the cells. Cells were either plated onto 35 mm glass bottom poly-d-lysine coated confocal dishes for real time functional imaging or were plated into 60 mm culture dishes holding a poly-l-lysine coated glass coverslip for fixed cell staining. All groups were either left untreated or treated with 0.5 mM DCA for 48 hrs at 37º C.

For real time functional imaging the differently treated groups were stained with either TMRM 10 nM for 30 minutes at 37º C and then washed with appropriate medium before imaging. Or they were stained with MITOSOX at 5 μM in serum free medium for 10 minutes and then washed with the appropriate medium. All were counterstained with 0.5 μM Hoechst for 10 minutes to stain the cell nuclei.

For fixed cell/tissue PDK II imaging, cells were fixed with 4% paraformaldehyde in medium for 15 minutes at 37º C. They were then washed with PBS and treated with Image-enhancer IT $_{TM}$ for 30 minutes at RT. The cells were then stained sequentially with PDKII (Santa Cruz) antibody 1:100 dilution for one hour at 37º C. The samples then received Alexafluor $_{TM}$ 488 (green) (Invitrogen) conjugated secondary antibody at 1:1000 dilution for one hour at 37º C. The cells were then counterstained with DAPI 0.5 μM for 10 minutes. The cover slips holding the adherent cells were then mounted to glass microscope slides with Prolong Gold $_{TM}$ anti-fade compound.

Live Cell Isolation from Tissue Samples:

Glioblastoma multiforme cells were isolated utilizing the following procedure: (*44*) Tumor specimens from adult GBM patients were received within 30 minutes of resection from surgery and maintained in ice cold RPMI1640 medium. The tumor cells were isolated using the Panomic Cancer Cell Isolation Kit (Fremont, CA, USA, Cat# CI0002). Intact, viable appearing tumor tissue was selected and cut into small pieces. The pieces were transferred to a 50mL falcon tube containing 20mL serum-free RPMI medium and centrifuged at 1200 rpm for 6 minutes, in a Sorvall Legend RT+ Centrifuge. The

supernatant was discarded and the tissue was enzymatically dissociated using 10mL of the Panomic Cancer Cell Isolation Kit tumor cell digestion solution at 37º C for 2 hours with gentle agitation. Another 10mL of tumor cell suspension solution was added, triturated and the solution was put through a 100 mm cell strainer into a 50mL falcon tube. The cells were centrifuged for 8 minutes at 1200 rpm and the supernatant was discarded. The cells were resuspended in the tumor cell suspension solution. The tumor cell purification solution was prepared by adding 20mL into a 50mL falcon tube, and centrifuging for 2 minutes at 1200 rpm. The cell suspension solution was carefully added by pipetting down the wall of the tube containing the purification solution, creating two layers of solutions. The tumor cells were allowed to settle for 6 minutes. From the bottom, 6mL of tumor suspension solution was collected and transferred to another 50mL falcon tube. The cells were pelletted by centrifuging for 8 minutes at 1200 rpm and then resuspended in DMEM/F12 media supplemented with 10%, 1% PSF, non-essential amino acids, 1mM sodium pyruvate and glutamine at a concentration of $2x10^6$ cells/$75cm^2$ flask. The cell lines were expanded while still low passage (i.e. p0-p1) and cryo-preserved in liquid N_2 to produce frozen stock.

Commercially Obtained Cryogenically Preserved Cells:

A vial containing frozen cells was removed from liquid nitrogen and quickly thawed, either by placing in warm (37º C) water bath or by being held in a gloved hand. To wash off the DMSO, a growth medium (approx 1 ml) appropriate to cell type was pipetted into the vial and cells were suspended by trituration. The cells were spun down and pelletted by centrifugation after which the supernatant was aspirated off. More growth medium (approx. 1.0 ml) was added and the cells were resuspended. The cells were then plated out into culture flasks of the desired type with the required growth medium. The cells were placed in a standard cell culture incubator under normal conditions (37º C) with appropriate N_2, O_2 and CO_2 gas mix. The culture flasks were checked the next day and the medium was replaced, this was repeated every two days. After this point, the procedure for commercially purchased and in-house isolated cell lines was similar.

Handling procedures for cultured cells:

When cells growing in flasks had reached the desired confluency, the growth medium was aspirated off and the adherent cells were rinsed with PBS sufficiently to remove all traces of medium. PBS containing trypsin of the appropriate type was added to the flasks

and allowed to react with the cells for the appropriate length of time to detach them. The flask was agitated to detach and suspend the cells and serum or complete medium was added to neutralize the trypsin. The suspended cells were transferred to 50 ml falcon tubes and pelletted by centrifugation after which the supernatant was aspirated off. The cells were then resuspended in fresh medium of the appropriate type. The cells were then either transferred to flasks for further growth or plated out into culture dishes of a type and size appropriate to the required experimental protocol. After this, the cells were returned to the incubator to reach the desired confluency. The adherent cells were checked every two days and the growth medium was replaced as required.

For functional imaging, the cells were seeded directly into MatTek 35mm poly-D-lysine coated glass bottom confocal dishes. For fixed cell imaging the cells were seeded into standard 60 mm dishes containing a poly-L-lysine coated glass coverslip of an appropriate size. When the cells had reached the required confluency, they were given the treatment of choice for the desired amount of time. The cells in the confocal dishes were stained with the chosen metabolic indicators (TMRM and Hoechst for example) and then imaged live on the confocal microscope. Further treatments could be added while the sample was on the microscope stage to view functional changes in real time. The cells grown on the coverslips where fixed in an appropriate manner (4% paraformaldehyde for example) and then treated with the desired antibodies and stained with the required fluorophores. After staining the coverslips were mounted on glass microscope slides with an antifade mounting compound like Prolong Gold $_{TM}$ (*45*). Static imaging was performed on the confocal microscope.

Functional Metabolic Indicator Dyes:

In the experiments presented in this thesis, three fluorescent indicators TMRM, MITOSOX and Hoechst 33342 were used to compare live cell metabolic processes between cancer and normal cells both with and without treatment by DCA. TMRM was used to compare the mitochondrial membrane potential ($\Delta\psi m$) and MITOSOX was used to compare mitochondria-derived reactive oxygen species (mROS). Nuclei were routinely stained using the nuclear DNA marker Hoechst 33342. In addition various antibodies and organelle stains (to be described later) were used to investigate fixed cells and tissues.

TMRM:

TMRM (tetramethylrhodamine methyl ester) (*46*) is a Δψm-sensitive indicator. This is an optically excited (laser 543 nm) red fluorescent (565-615 nm bp emission filter) dynamic dye which is attracted to the negative inner membrane potential of the mitochondria and indicates an increase or decrease in Δψm. Being a dynamic indicator the fluorescence can continuously brighten and dim as Δψm changes and the comparison of the relative fluorescence can give an indication of the relative Δψm between cells.

TMRM is a relatively non-toxic cationic (positively charged) lipophilic rhodamine dye which is able to selectively stain the mitochondria of living cells at low concentrations, although at higher concentrations it can also accumulate in the endoplasmic reticulum.

It was shown that the accumulation of TMRM in mitochondria is driven by the mitochondrial membrane potential (Δψm) (*47*). When TMRM is attracted to the negative potential within the inner membrane of the mitochondria it is absorbed spanning both the inner and outer aspect of the inner membrane (*48*). TMRM is rapidly and reversibly taken up by live cells and has been used to dynamically measure time dependant changes in the Δψm (*48*) (hyper-polarization and depolarization) of the mitochondria such as after changes in cytosolic Ca_{2+} transients. In my experiments TMRM was used to measure Δψm depolarization related to the opening of the mitochondrial transition pore after treatment with DCA. TMRM loading is temperature sensitive and decreases as temperature decreases. TMRM in high concentration stains endoplasmic reticulum and can affect mitochondrial membrane potential, but displays no toxicity at levels normally used (around 10 nM).

Mitotracker Red CMX Ros:

Mitotracker Red **(**46**)** is a fixable cell permeant probe selective for active mitochondria as it is sensitive to the Δψm. It is added to the cell culture solution in submicromolar concentrations and incubated with the cells, passively diffusing through the cell membrane and accumulating in the mitochondria. It binds exclusively to actively respiring mitochondria (partially dependent on the Δψm) but remains bound after the loss of the Δψm through the action of a mildly a thiol-reactive chloromethyl moiety which is responsible for keeping it attached to the mitochondria after aldehyde fixation. Subsequent permeabilization of the cell membranes for further staining does not affect the mitochondrial staining pattern. It has an excitation maximum at 578 nm but the 548

nm laser line is used with this confocal system as the 578 nm line is not available and in any case would have overlapped with the emission spectrum (565-615 nm).(*46*)

MITOSOX:

MITOSOX (mitochondrial superoxide indicator) (*46*) a derivative of hydroethidine, is an optically excited (laser 400 and 514 nm), red fluorescent (565-615 nm emission bp filter) indicator of the ROS produced by the mitochondria. This is a non-dynamic indicator which reacts to the maximum amount of superoxide and other reactive oxygen species produced by becoming oxidized and thus changing from colorless (membrane permeable) to red (membrane impermeable). Being non-dynamic, once oxidized it cannot revert back to the colorless permeable form even if the concentration of reactive oxygen species decreases. MITOSOX is used for the detection of superoxide derived from the mitochondria in living cells. It consists of a cationic hexyltriphenylphosphonium derivative of dihydroethidium (Mito-HE) which is electrophoretically taken up by actively respiring mitochondria. When oxidised in mitochondria Mitosox becomes red in color. When superoxide (but not other reactive oxygen species) oxidizes the dihydroethidium component of MITOSOX, hydroxylation of the 2-position occurs resulting in the 2-hydroxyethidium derivative of MITOSOX. This derivative, but not those produced by other reactive oxygen species, display an excitation peak at about 400 nm and produce a fluorescence peak at around 590 nm. Excitation at 514 nm also produces red fluorescence at 590 nm but is less discriminating, displaying the products of other reactive oxygen species along with the superoxide product.(*49, 50*)

Because MITOSOX is a derivative of dihydroethidium it binds with DNA at high concentrations, staining the nucleus red. Sensitive to air (O_2) and light it will spontaneously oxidize (*46*). So when preparing it the microtubes used to hold the aliquots should be wrapped with aluminum foil, purged under N_2 gas flow to exclude as much oxygen as possible and then frozen at -20ºC or lower until ready to use.(*49*)

In my experiments MITOSOX was used to measure changes in mROS related to treatment with DCA and was imaged at 514 nm and so potentially displayed the contribution of other reactive oxygen species like H_2O_2 (which is the result of the dismutation of superoxide by superoxide dismutase).

Hoechst 33342:

Hoechst 33342 (*46*) is a water soluble bis-benzimide derived DNA specific dye (*46*). It is live cell permeant and is used to stain the nuclei of cells (live or fixed). Hoechst 33342 is UV (350 nm) excited and fluoresces a blue/cyan (461 nm) colour when bound to DNA. In its unbound state it has a maximum fluorescence emission between 510-540 nm (green) but when bound to DNA it undergoes a fluorescence shift to 461 nm peak emission. Hoechst is extremely useful for multiple fluorophore imaging protocols because of the strong Stokes shift between the excitation and emission spectra. Hoechst 33342 can bind to all nucleic acids but binds preferentially to adenine and thymidine (AT) rich sequences within the minor groove of double stranded DNA, causing a considerable enhancement in fluorescence over Hoechst bound to other nucleotide sequences. When used under normal loading conditions at a concentration of around 500 nM for 5 to 30 minutes at 37ºC, it does not affect the short term viability of cells. After the Hoechst loading medium is washed off its fluorescence may diminish over time as it is actively transported out of the cell. In all the experiments presented in this document two-photon excitation at 740 nm was used for the excitation of Hoechst and its fixed cell staining counterpart DAPI. Hoechst is mutagenic and carcinogenic and can interfere with cell replication because of its binding to DNA and therefore must be used at low concentrations. When used at too high a concentration the green fluorescence of unbound Hoechst can become apparent within the cytoplasm of loaded cells.(*46*)

DAPI:

DAPI (4',6-diamidino-2-phenylindole dihydrochloride)(*46*) is the fixed sample counterpart of the nuclear stain Hoechst, with similar fluorescence properties. It is only semi-permeant to live cell membranes and takes longer to stain nuclei than Hoechst so it is most often used for fixed (permeablized cell) staining. Like Hoechst, Dapi is mutagenic and carcinogenic and can also interfere with cell replication. Dapi like Hoechst must be used at low concentrations so if used in live cell imaging its lower permeability means that it takes longer to stain, making Hoechst the preferable choice for this purpose.(*46*)

Fixed tissue and cell Imaging:

In addition to functional imaging of live cells or tissues, changes in metabolic processes like enzyme activity and changes in physical structures such as membranes or organelles

can be investigated in fixed samples as well. Visualization may be accomplished with immuno-staining techniques using antibodies or with non-immuno techniques which use indicators which are specific to certain molecular, electrochemical or structural attributes of the organelle or process being investigated. Cells or tissues may be stained while alive and then fixed (post-fixed) to arrest a metabolic process or to preserve a structure for later imaging. Likewise, the cells or tissue may be fixed first (prefixed) to preserve the localization of antigens or structures and then stained after fixation to visualize the subject of interest. In the immuno-techniques, however, pre-fixation (especially in formalin fixed paraffin embedded samples) may add some complications to the staining process in that it may mask the antigens of interest rendering them unrecognizable to the primary antibodies. This requires an extra antigen retrieval step (to be described in more detail) for unmasking to allow for successful identification.

Immuno Staining Techniques:

Immunological techniques for two main methods (fluorescent and non-fluorescent) exist for both cells and tissues. Staining cells is called immunocytochemistry and staining tissues is called immunohistochemistry. For non-fluorescent visualization a chromogenic technique is used. For the immunofluorescence technique a fluorescent conjugate is used. Both techniques utilize a primary antibody which recognizes the antigen of interest but differ in how it is visualized.

Two Step Process:

In this technique after the primary antibody has bound to the antigen of interest a secondary antibody pre-conjugated with a fluorescent fluorophore is added. The secondary antibody recognizes and binds to an immunological marker (IGg) on the primary and this tags the primary with the fluorophore. The immunological marker is derived from the host that the primary antibody was developed in, rabbit for example. The secondary antibody is produced from a different host animal, goat for example which is immunized against the immunological marker (IGg) of the primary host. The disadvantage here is that the sample being stained must not be from the same type of animal host that the primary antibody was developed in. If the sample and host of the primary antibody are the same kind of animal (rabbit for example) the secondary antibody (goat anti-rabbit IGg) will react to the sample IGg as well as the primary antibody IGg causing everything to fluoresce and masking the signal from the antigen of

interest. In fact the species of host that the primary is raised in should be as phylogenetically different from the species being investigated as is possible. An antibody produced in mouse might cause cross reaction if used to stain rat samples as they are quite close genetically, chicken or goat would be a better choice. Furthermore, the primary antibody should be produced against an antigen derived from the species under investigation. For example when staining for an antigen of human origin (like phosphodiesterase V) the antigen used to produce the primary should also be derived from human samples. When antigens are highly conserved between species (like smooth muscle actin for example) this requirement is not as stringent(*46*), (*51*).

The advantage of the two step process is that when host specificity is properly accounted for, multiple fluorophore tagged secondaries can bind with the primary producing a very bright signal. The fluorophore tagged antibody can then be visualized on a confocal or standard fluorescence microscope as a fluorescent signal of various colors, often some shade of red or green but other colors are available as well. This is a simpler staining technique than the non-fluorescent method because only a primary and its secondary antibody are used with no intermediate immunochemical steps required. Because secondary antibodies conjugated with various fluorophores of different colors are available, multiple antigens may be visualized on the same sample simultaneously.
This is the technique which was used for most of the fixed cell or tissue experiments.

Preconjugation:

It is possible to pre-conjugate the primary antibody with a fluorescent secondary antibody before adding it to the sample being investigated. This allows multiple primary antibodies produced from the same animal host to be used simultaneously on the sample under investigation. Primary antibodies may be purchased which are already pre-conjugated with a fluorophore or one can perform the pre-conjugation step before adding the primary antibody to the sample under investigation. Various kits from companies like Molecular Probes (Invitrogen) and Vector Technologies are available which allow one to take any primary antibody of choice and conjugate it using the appropriate labelling reagent. They use a fluorescently labelled Fab fragment to bind with the Fc portion of the IgG primary antibody. Any excess Fab fragment is neutralized by a non-specific IgG which acts as a blocking agent to prevent any further binding with other primary antibodies of the same type. The brightness of the fluorescence signal can be increased

by increasing the ratio of labelling reagent to primary antibody. The labelling procedure usually takes only about 10 minutes in total. The cost of these kits is higher than for the standard two step process however.

Single Step Process:

This is the simplest staining technique because the primary antibody is purchased already conjugated with its fluorophore and since no secondary antibody is required there is no problem with sample/host antibody interaction. Although less time consuming than the two step process it has the disadvantage of not producing as bright an image. This is because fewer fluorophore molecules are conjugated onto each primary antibody. As with the two step process various fluorophores of different colors are available so multiple antigens may be visualized on the same sample. Pre-conjugated primaries tend to be more expensive than the un-conjugated ones.

Non-immuno Staining Techniques:

Non-immunological staining methods differ from immunological techniques in that no anti-bodies are used. A non-immunological stain which is specific to some chemical or structural property of cells or tissue is utilized. Again as with immuno-staining techniques there are fluorescent and non-fluorescent methods of visualization. As with immunological techniques non-immuno methods can be used with either live or fixed specimens. However, some non-immuno staining protocols can only be carried out while the specimen is still alive and fixation may then be done after staining is complete. An example is Mitotracker Red which can only be used to stain mitochondria within live cells (it is $\Delta\psi m$ sensitive) but can subsequently be fixed to permanently preserve the staining of the mitochondrial morphology and distribution. Some non-immuno stains can also be applied to samples that are already dead and fixed such as the blue nuclear stain Dapi (the fixed cell counterpart of Hoechst) while still displaying very good visualization of morphology, localization etc.

Hematoxylin and Eosin (H&E):

H&E staining is a standard non-fluorescent technique used to visualize the structures of tissues (e.g. blood vessels or lung airways) as well the localization of nuclei with the use of a standard light microscope. Eosin Y (eosin yellowish) is the tetrabromo derivative of fluorescein and eosin B (eosin bluish) is the dibromo derivative of fluorescein. Although

it is used for non-fluorescence imaging, being a derivative of fluorescein it is fluorescent when properly excited. Depending on the concentration eosin Y can take on a yellow to orange color in solution (either ethanol or water) and eosin B can take a bluish to scarlet color. They both stain muscle fibres as well as the cytoplasm and collagen in structures such as lung airways and blood vessels in shades ranging from an orange to pink to red and red blood cells an intense shade of red. Being acidic eosin is found to stain the basic parts of cells and tissues and does not stain acidic components like DNA. To obtain a stronger eosin stain **eosin with phloxin** can be used but this may produce too strong a pinkish/red hue for some tastes and is a matter of personal preference.

Hematoxylin is an extract of the heartwood of the logwood tree which is found in Central and South America. In its oxidized form it forms complexes with iron or aluminum producing very strongly coloured products (blue-white for aluminum and blue-black for iron). Being basic it stains the acidic components of tissues and cells, staining RNA and DNA in nuclei a blue-black to purple color. H&E is used exclusively with fixed tissues and is not sensitive to the type of fixation used providing that the fixation method preserves the morphology of the sample. It can be used in conjunction with immunohistochemistry as a counter stain to show the localization of a specific antigen (usually as some shade of brown) within the structures of the tissues.

Tissue Fixation and Processing Methods:

As was mentioned in the previous section the success of some staining methods are sensitive to the type of fixation used for a specific sample. There are number of types of fixation to choose from and the choice of a specific method depends on what type of cells, tissues or staining methods are of interest (*51*)**:**.

Paraffin Sections:

The fresh tissue is first fixed in a solution like 10 % formalin or SafeFix$_{TM}$ and then processed in a paraffin tissue processor. The time for fixation depends on the density and thickness of the tissue, but it is important not to over-fix as this will toughen the tissue and overly mask the antigens of interest (by formation of methylene cross links). The formalin fixation could last anywhere from a few hours to a week or more, but if long term storage without further processing is required the sample should be transferred to 70% ethanol when sufficiently fixed. It can be stored this way for a considerable time (up

to many years). If the tissue is processed by paraffin infiltration it will be permanently preserved in a wax block and can be stored indefinitely. However, formalin fixation and paraffin embedding will often mask antigens and an extra antigen retrieval step is required to unmask the antigens before immuno-staining can be done. When the sample is required for staining, the wax block containing the embedded tissue is placed on a microtome and slices of the appropriate thickness are cut and floated on a warm (400 C) water bath to facilitate transfer onto Superfrost$_{TM}$ (or other appropriately coated) microscope slides. The coating on the slides provides a charged surface to which the tissue sections will adhere strongly. Slides are heated overnight (48.5º C) to dry and adhere the wax slices to the glass. After drying the samples must be dewaxed and brought to aqueous solution before staining can occur. From this point on they must not be allowed to dry out. If immunostaining is to occur the slides must be subjected to an antigen retrieval process. This can be done by various methods. The two most common methods are heat induced and enzymatic epitope retrieval. A common method used is to heat (not boil!) the slides at 95-98º C in a 10 mM citric acid /citrate buffer for about 15-20 minutes in a microwave oven or steamer or alternatively the samples may be heated for 2-5 minutes in a pressure cooker (122º C). The heating times for both methods can vary and must be initially determined by trial and error. The heating process breaks the methylene cross link bridges and exposes the antigens to the antibodies.

Another method commonly used is enzymatic, whereby a proteinase (trypsin, pepsin or proteinase K) solution (concentration depending on the choice of enzyme) is applied to the samples for about 5-20 minutes at 37ºC in an incubator to perform a mild digestion. This also exposes the antigens by breaking the methylene cross links but is time sensitive as over-digestion could degrade the sample. After this the tissue is rinsed with PBS to wash off the enzyme. Whatever method is chosen, from this point on the tissue is suitable for the desired staining protocol.

Frozen Sections:

If formalin fixation with paraffin embedding is not desired, the fresh tissue can be flash frozen, embedded in a polyvinyl alcohol based sectioning medium such as OCT and while still frozen sectioned onto microscope slides using a cryostat. The tissue slides are then kept frozen until required and thawed and fixed just before use. The choice of fixative depends on the specific application. A common choice which preserves

morphology and does not overly mask the antigens is 4% paraformaldehyde for 10 minutes. Alternatively ice cold (-10º C) acetone or alcohol may be used as this does not mask antigens but may cause poor preservation of nuclear morphology. Frozen sections are the easiest and quickest to stain as no dewaxing or antigen retrieval step is required.

B3. Results

In collaboration with the Division of Neurosurgery at the University of Alberta, biopsies were received from 8 separate glioblastoma multiform (GBM) patients and normal brain tissue biopsies from 3 separate epilepsy patients (Fig. 12A)(*1*). To determine if dichloroacetate (DCA) may be a valid therapy for GBM , PDKII expression (the isoform of PDK most sensitive to DCA) was measured first in normal and GBM tissues. PDKII expression was significantly increased in GBM tissues compared to normal healthy brain tissues using both immunofluorescence (Fig.12B) (*1*) and immunoblots (Fig.12C)(*1*).

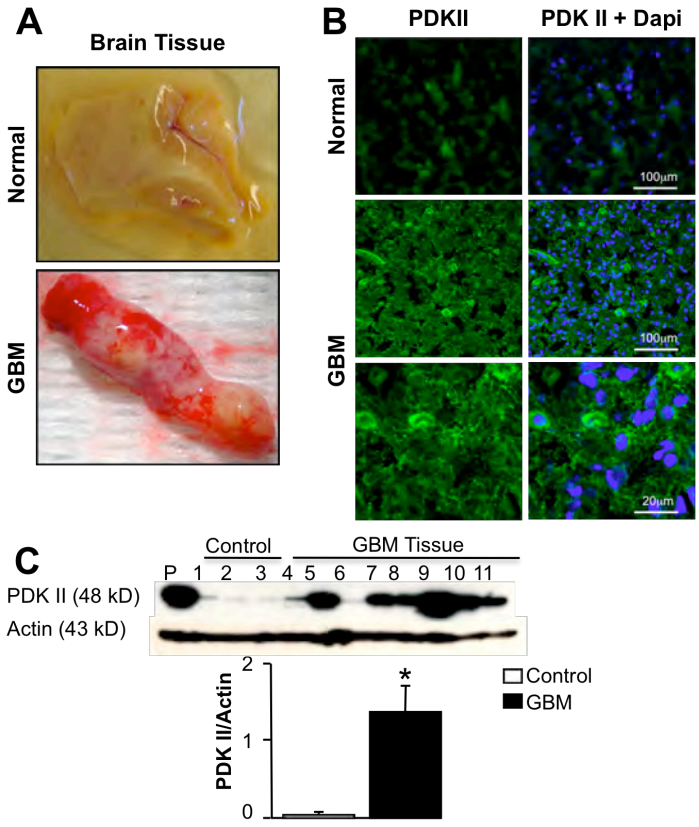

Figure 12: A comparison of PDK expression between normal brain and GBM tissue. (A) The mitochondrial enzyme PDKII, which is the target of DCA is highly expressed in human GBM tumors compared to non-cancerous brain tissue obtained from epilepsy surgery. (B) Representative images of PDKII (shown in green) nuclear stain DAPI (shown in blue). (C) Immunoblots are shown along with mean data normalized to actin. N=3 $P<0.05$

The functional effects which DCA would have on mitochondrial membrane potential (ΔΨm) and mitochondrial-derived reactive oxygen species (mROS) was examined next. GBM biopsies from 40 consecutive patients were obtained (summarized in Fig. 13) from the operating room within 20 minutes of removal following tumor debulking surgery. Using TMRM (as previously described) and confocal microscopy mitochondrial ΔΨm was measured before and after acute treatment of GBM and normal brain tissues with DCA. While DCA had no effects on ΔΨm of normal brain tissues (Fig.14)(*1*), it significantly depolarized ΔΨm of GBM tissues (Fig.14 and Table 1) (*1*), where PDKII was shown to be highly expressed (Fig.12)(*1*). In addition, GBM tissues had increased ΔΨm compared to normal brain tissues, suggesting that mitochondrial function (GO) is suppressed in these tumors (Fig.14).

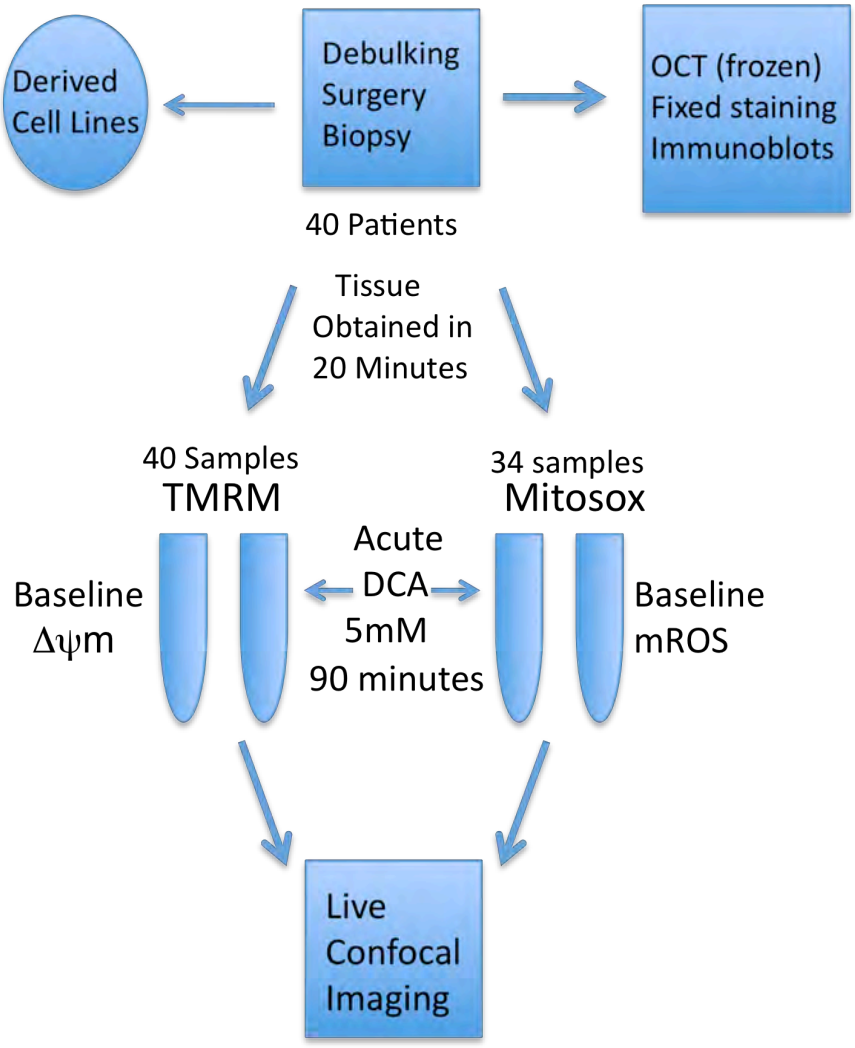

Figure 13: Summary diagram of surgical tissue acquisition and usage

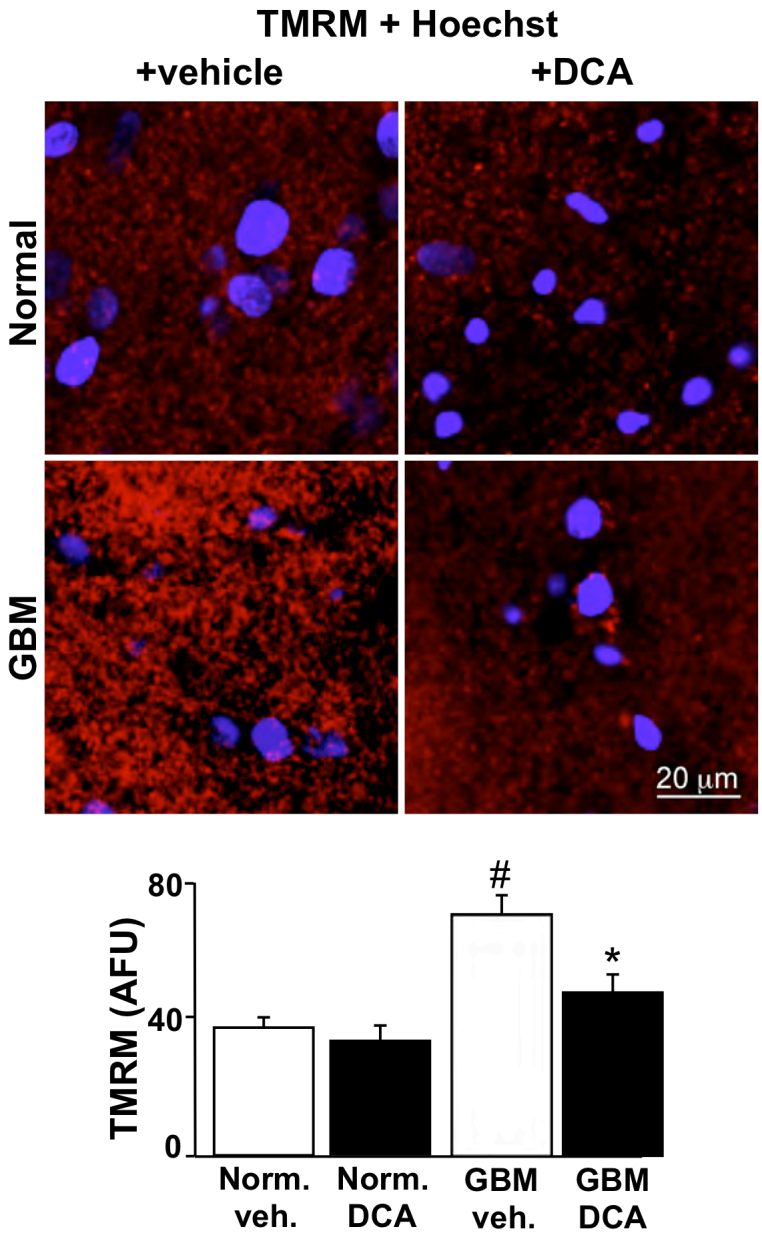

Figure 14: Acute DCA studies of freshly isolated tissue.
Tissue was maintained at 37º C, within 20 minutes of extraction in the operating room. Representative photomicrographs indicating mitochondrial membrane potential as measured with TMRM (red) along with nuclear stain Hoechst (blue) are shown along with mean data from tissue derived from patients shown in table 1. Arbitrary fluorescence units (AFU) are reported. N=40 $P<0.05$

Note that for all figures the confocal fluorescence quantifications of TMRM and Mitosox are presented as Arbitrary Fluorescence Units (A.F.U).

Table 1: Study of Δψm (TMRM A.F.U) in live GBM tissue derived from 40 Glioblastoma patients.

Patient #	Control	DCA	Patient #	Control	DCA
1	91 ± 3.59	69 ± 4.12	**21**	15 ± 3.80	10 ± 2.60
2	28 ± 2.28	19 ± 0.98	**22**	109 ± 5.10	80 ± 6.00
3	92 ± 3.86	28 ± 2.01	**23**	11 ± 3.50	4.3 ± 1.70
4	30 ± 1.94	30 ± 1.52	**24**	66 ± 2.90	9.6 ± 2.20
5	50 ± 3.31	41 ± 3.28	**25**	43 ± 2.68	33 ± 2.03
6	69 ± 6.60	38 ± 2.90	**26**	36 ± 3.90	23 ± 1.24
7	59 ± 4.30	18 ± 1.10	**27**	44 ± 3.40	34 ± 7.60
8	38 ± 2.46	17 ± 1.33	**28**	69 ± 4.90	39 ± 2.35
9	52 ± 3.65	42 ± 3.88	**29**	45 ± 6.00	27 ± 2.00
10	58 ± 5.5	37 ± 3.25	**30**	53 ± 4.30	44 ± 3.40
11	34 ±3.46	54 ± 5.15	**31**	27 ± 2.60	28 ± 3.01
12	49 ± 7.47	54 ± 12.52	**32**	51 ± 4.10	31 ± 4.67
13	96 ± 5.6	45 ± 4.10	**33**	56 ± 6.30	38 ± 3.12
14	172 ± 8.35	176 ± 8.00	**34**	109 ± 8.00	50 ± 4.00
15	85 ± 5.96	47 ± 4.10	**35**	146 ± 6.20	73 ± 4.90
16	62 ± 5.00	52 ± 3.00	**36**	47 ± 1.30	37 ± 1.30
17	157 ± 7.89	114 ± 6.85	**37**	142 ± 3.40	56 ± 4.40
18	60 ± 4.70	41 ± 1.80	**38**	93 ± 7.50	40 ± 2.00
19	110 ± 5.70	74 ± 3.01	**39**	54 ± 3.40	22 ± 1.20
20	40 ± 2.45	28 ± 1.76	**40**	105 ± 10.30	86 ± 7.90

Tissues were obtained with 20 minutes of surgery and either left untreated or treated acutely with DCA for 2 hours and then stained with TMRM to measure Δψm.

To further assess the effects of DCA on mitochondrial function mROS was measured in 34 of these same GBM tissues (since limited tissue was obtained from 6 patients, priority was given for TMRM) using the mitochondrial reactive oxygen (mROS) specific dye MITOSOX. Acute treatment with DCA increased mROS levels in GBM tissues compared to vehicle (Fig.15 and Table 2)(*1*).

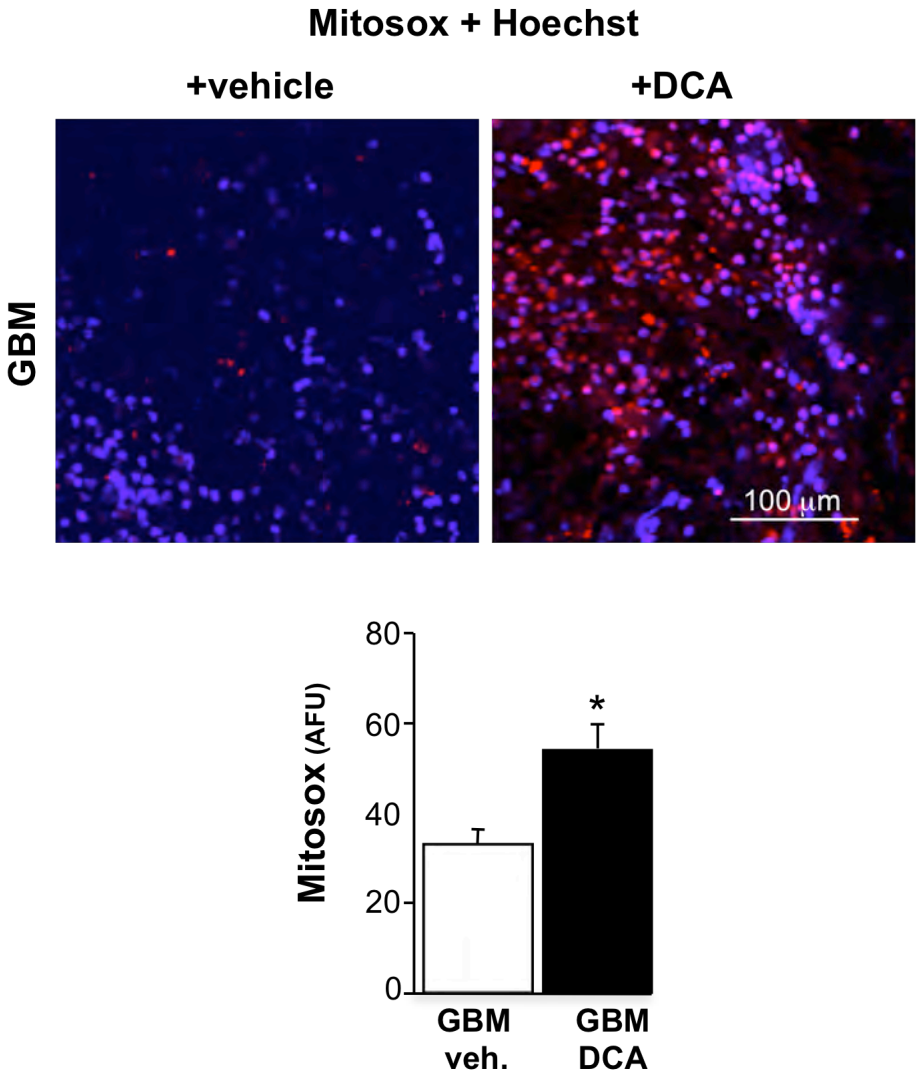

Figure 15: Study of acute DCA effects on mROS (Mitosox) in freshly isolated tissue. Tissue was maintained at 37º C, within 20 minutes of extraction in the operating room. Representative photomicrographs indicating mitochondrial reactive oxygen (ROS)as measured with Mitosox (red) along with nuclear stain, Hoechst (blue) are shown along with mean data from tissue derived from patients shown in table 2. Arbitrary fluorescence units (AFU) are reported. N=34 $P<0.05$

Table 2: Study of mROS (Mitosox A.F.U.) in live GBM tissue derived from 34 Glioblastoma patients.

Patient #	Control	DCA	Patient #	Control	DCA
1	116 ± 6.86	218 ± 4.18	**21**	117 ± 5.60	122 ± 4.60
2	64 ± 3.67	66 ± 3.02	**22**	142 ± 6.30	113 ± 4.20
3	162 ± 5.05	79 ± 4.41	**23**	54 ± 5.30	96 ± 5.50
5	134 ± 5.04	183 ± 6.69	**24**	106 ± 7.70	147 ± 9.30
7	20 ± 6.30	43 ± 2.22	**25**	107 ± 7.10	129 ± 8.30
9	33 ± 3.23	54 ± 5.15	**26**	59 ± 3.83	67 ± 3.57
10	77 ± 8.67	50 ± 6.33	**27**	30 ± 2.04	15 ± 1.49
11	47 ± 4.32	75 ± 4.10	**28**	39 ± 6.47	35 ± 5.63
12	43 ± 3.15	70 ± 5.61	**29**	56 ± 5.04	72 ± 4.49
13	15 ± 2.00	68 ± 3.20	**30**	16 ± 1.90	29 ± 2.35
14	97 ± 7.12	109 ± 6.32	**31**	14 ± 0.65	15 ± 0.85
15	34 ± 3.43	44 ± 2.97	**32**	42 ± 4.43	92 ± 7.13
16	43 ± 2.87	40 ± 3.50	**33**	24 ± 1.60	44 ± 3.40
17	101 ± 9.22	75 ± 3.70	**37**	55 ± 5.50	60 ± 3.70
18	46 ± 5.30	116 ± 7.6	**38**	64 ± 5.70	122 ± 9.90
19	72 ± 6.30	136 ± 8.00	**39**	35 ± 3.90	58 ± 4.30
20	95 ± 3.60	145 ± 5.00	**40**	41 ± 1.80	39 ± 3.30

Tissues were obtained within 20 minutes of surgery and either left untreated or treated acutely with DCA for 2 hours and then stained with MITOSOX to measure mROS. Note: These are the same patients as shown in table 1 however patients 4,6,8,34,35,36 were not included because insufficient tissue was obtained to do both TMRM and Mitosox staining. To further characterize the effects of DCA on GBM and to validate the acute experimentswith TMRM and MITOSOX, primary cell lines were established from GBM tissues (summarized in Fig.16). Similar to the acute studies on GBM tissues, chronic treatment with DCA for 48 hrs, depolarized $\Delta\Psi m$ (Fig. 17A)(*1*) and increased mROS (Fig. 17B)(*1*) on primary GBM cell lines as well.

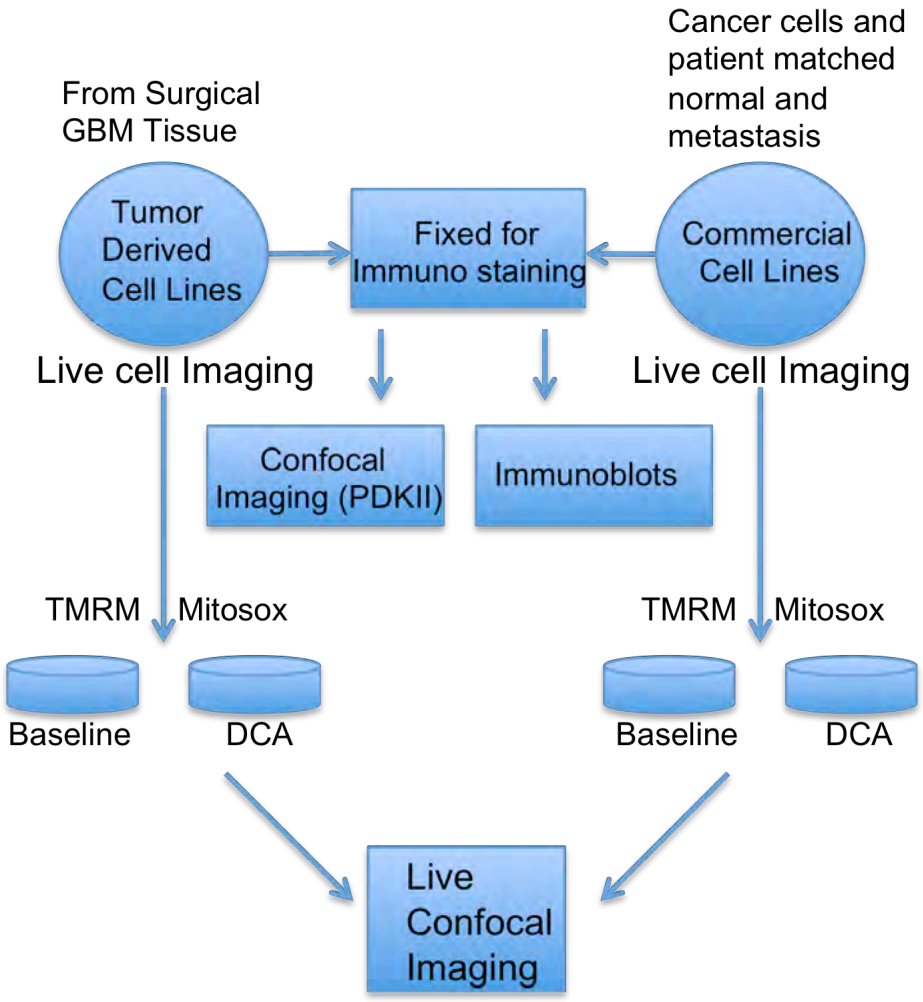

Figure 16: Summary diagram of commercial and GBM derived cell line utilization.

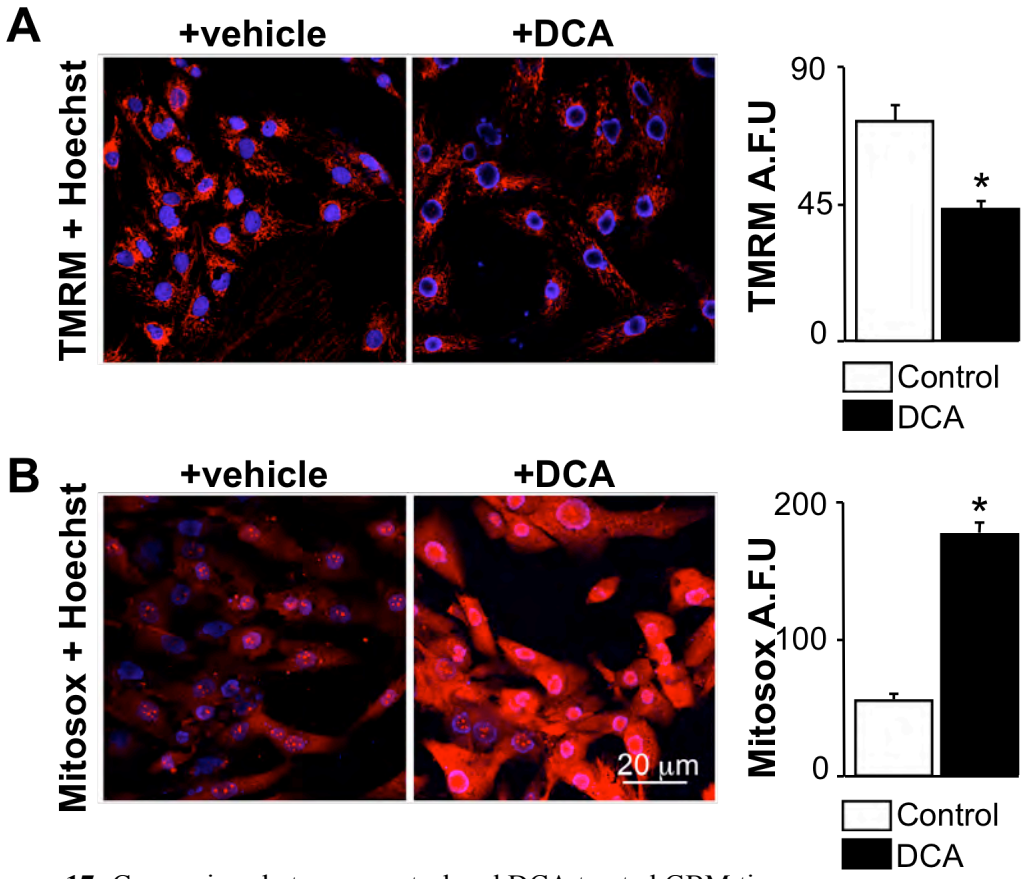

Figure 17: Comparison between control and DCA treated GBM tissue.
In primary GBM cell lines developed from GBM tumors, DCA decreases TMRM and increases Mitosox signal, consistent with its effects on the parent tissue of these cells. N=50 cells. $P<0.05$

To determine if confocal microscopy and live cell imaging can be extrapolated to other cancers, I obtained several commercially available cell lines derived from various solid tumors. Consistent with the primary GBM tumors, cell lines derived from lung cancer, melanoma, mammary carcinoma, metastatic lymph cancer and colorectal cancer highly expressed PDKII compared to a non-cancerous normal cell line (small airway epithelial cells, SAEC) (Fig. 18).

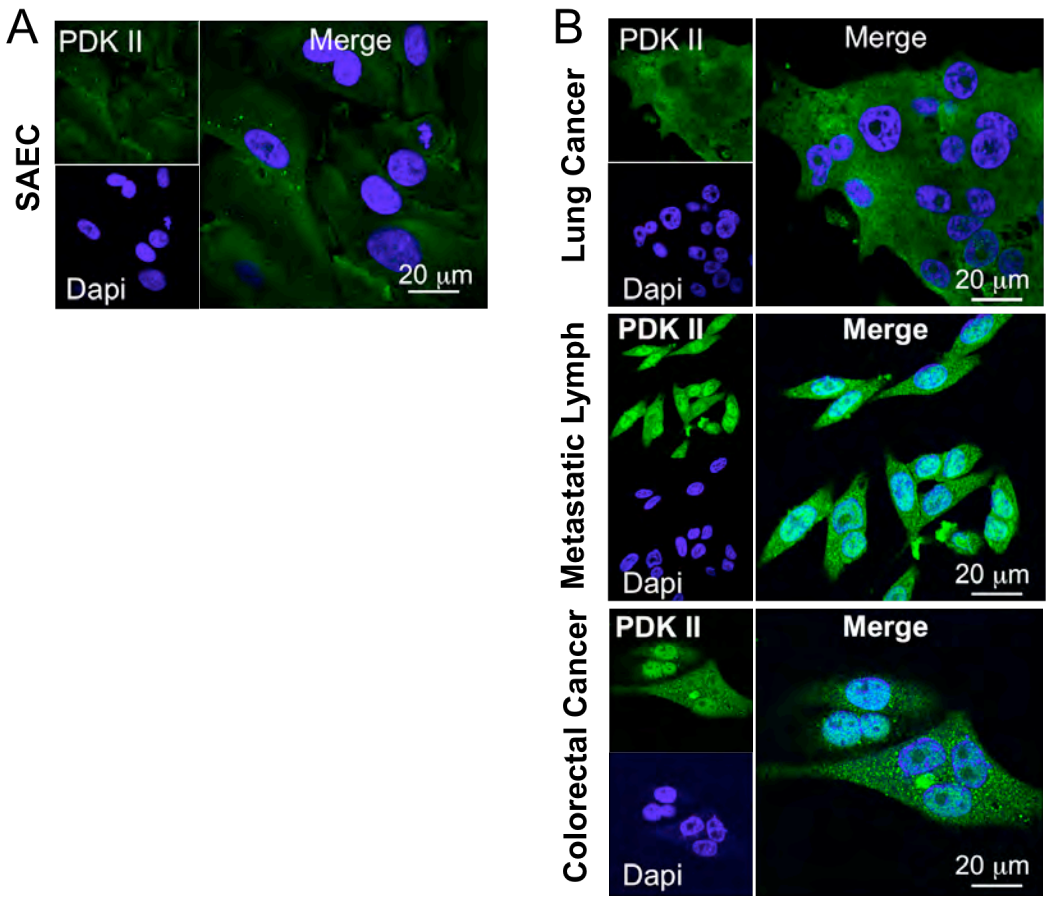

Figure 18: Comparison of PDKII expression between cell lines
Like in human GBM (Fig.11), PDK II is expressed in 3 different cancer lines at much higher levels compared to a normal epithelial cell line (small airway epithelial cells, SAEC).

Although DCA-treatment for 48 hrs did not have any effects on ΔΨm of normal SAECs, DCA significantly depolarized ΔΨm in lung cancer cells (Fig. 19). Similar to our GBM tissues, lung cancer cells had increased ΔΨm compared to normal SAECs, confirming that these cancer cells have suppressed mitochondrial function.

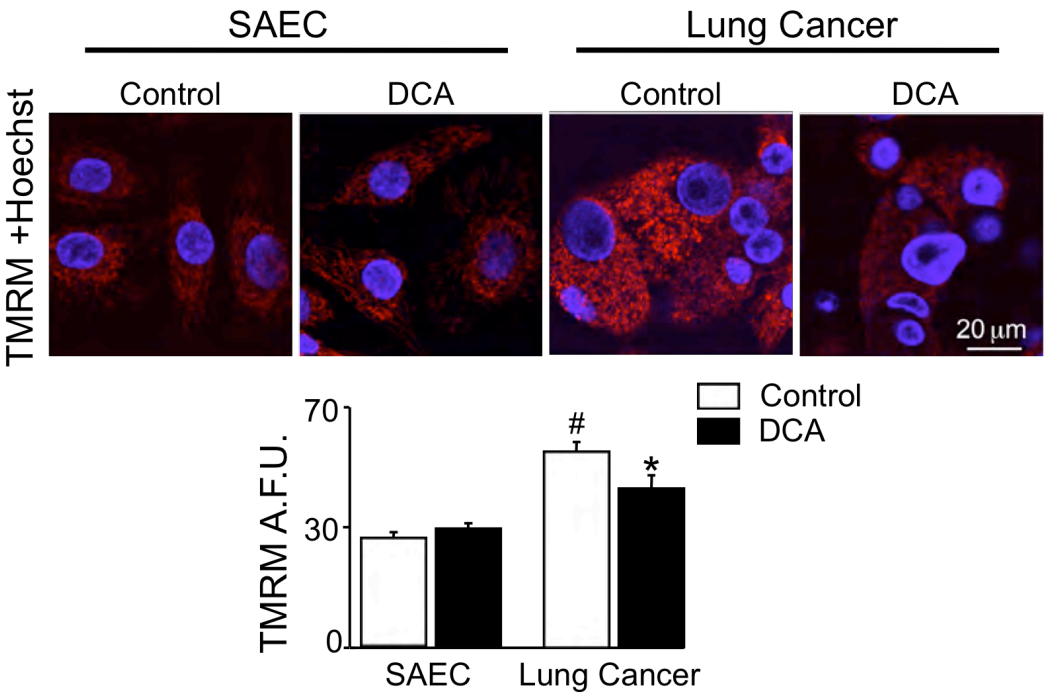

Figure 19: Comparison of DCA effects on ΔΨm between SAEC and lung cancer
Lack of DCA effects on TMRM on SAEC is associated with lack of the target enzyme (PDK II). DCA decreases TMRM fluorescence in a "PDK II-high" cancer cell line. N=50 $P<0.05$

It was seen that DCA had no effects on mROS production of normal SAECs (where PDKII is not highly expressed), but significantly increased mROS in lung cancer cells (Fig. 20). In addition, baseline mROS production was much less in the cancer cells than the normal SAECs, once again alluding to these cells having suppressed mitochondrial function (GO) (Fig. 19).

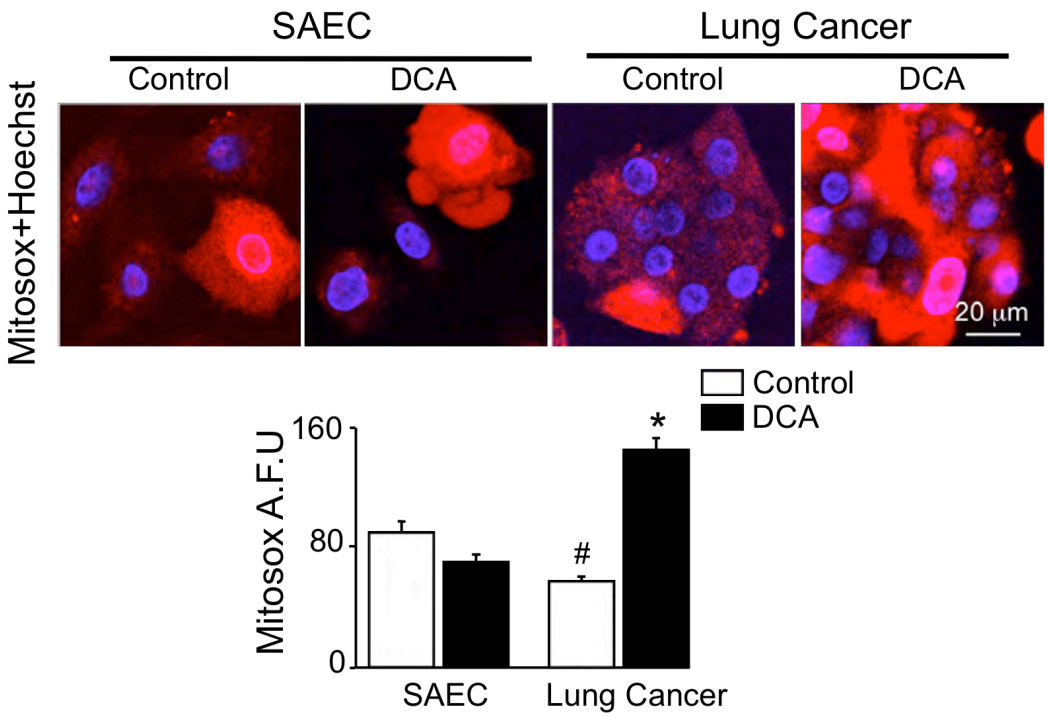

Figure 20: Comparison of DCA effects on mROS between SAEC and lung cancer. Lack of DCA effects on MITOSOX in SAEC is associated with lack of the target enzyme PDK II (Fig.15) N=50 P<0.05

DCA increases MITOSOX fluorescence in a "PDK II-high" cancer cell line. Similar results were also obtained when the effects of DCA on ΔΨm and mROS were compared in normal mammary fibroblasts and mammary carcinoma (Figs. 21 and 22).

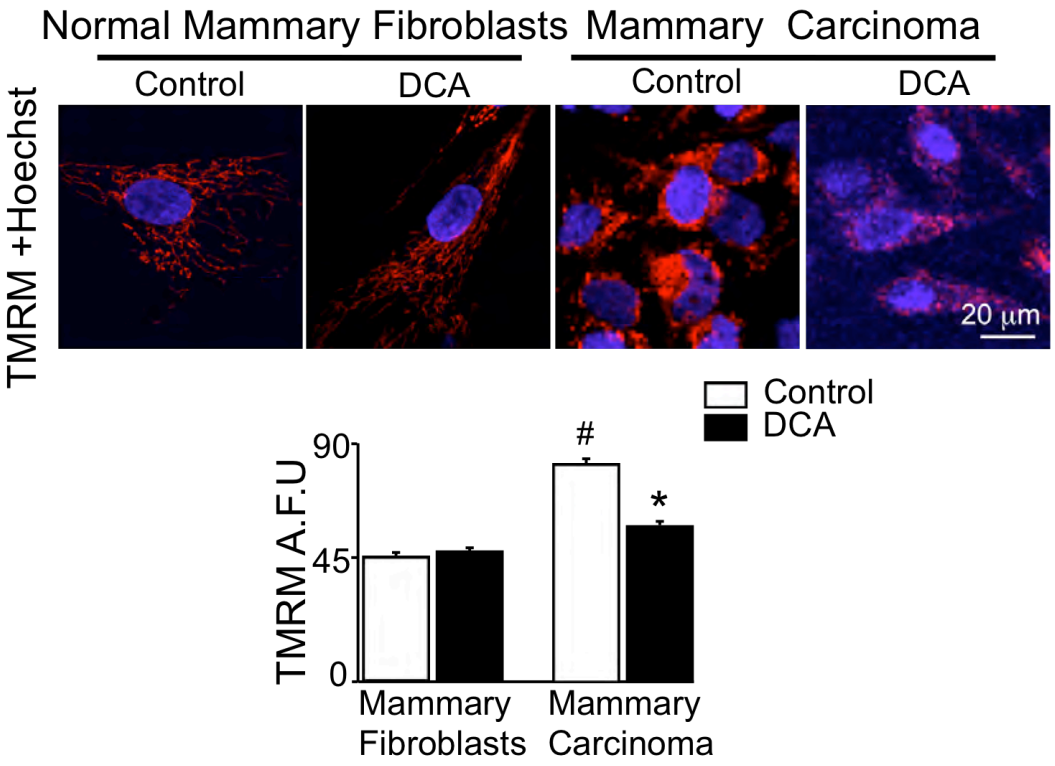

Figure 21: Comparison of DCA effects on ΔΨm between commercially available normal breast fibroblasts versus adenocarcinoma cells from the same patient.
Note the much higher ΔΨm in the cancer cells and its decrease by DCA, which is absent in normal, cells (both cell lines studied under identical conditions. N=50 $P<0.05$

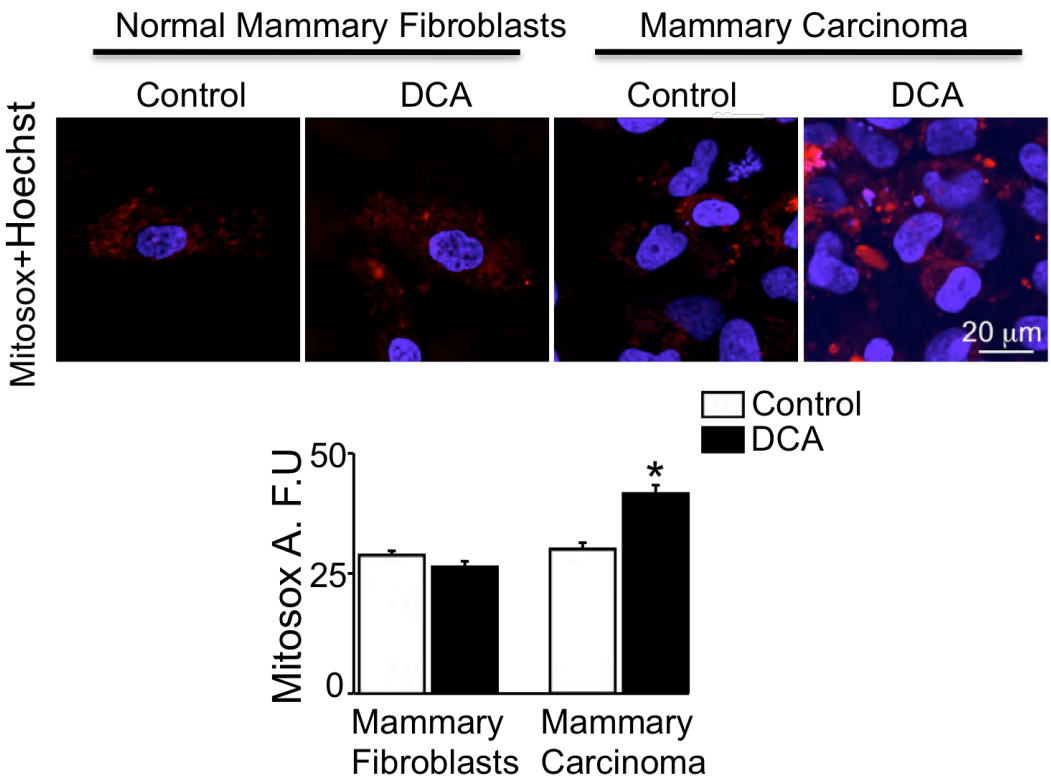

Figure 22: Comparison of DCA effects on mROS between commercially available normal breast fibroblasts versus adenocarcinoma cells from the same patient.
Note the similar amount of ROS in the untreated cancer cells and the normal cells and the increase in ROS in cancer by DCA which is absent in normal cells (both cell lines studied under identical conditions.) N=50 $P<0.05$

I next investigated if confocal microscopy and live cell imaging with TMRM and MITOSOX could be used to illuminate differences between a primary tumor and its corresponding metastatic tumor. I obtained commercially available cell lines from primary melanoma cancer cells and the corresponding metastases of the lymph derived from the same patient. Although baseline $\Delta\Psi m$ was not different between the primary and metastatic cell lines, DCA significantly depolarized both cancer cell lines (Fig. 23).

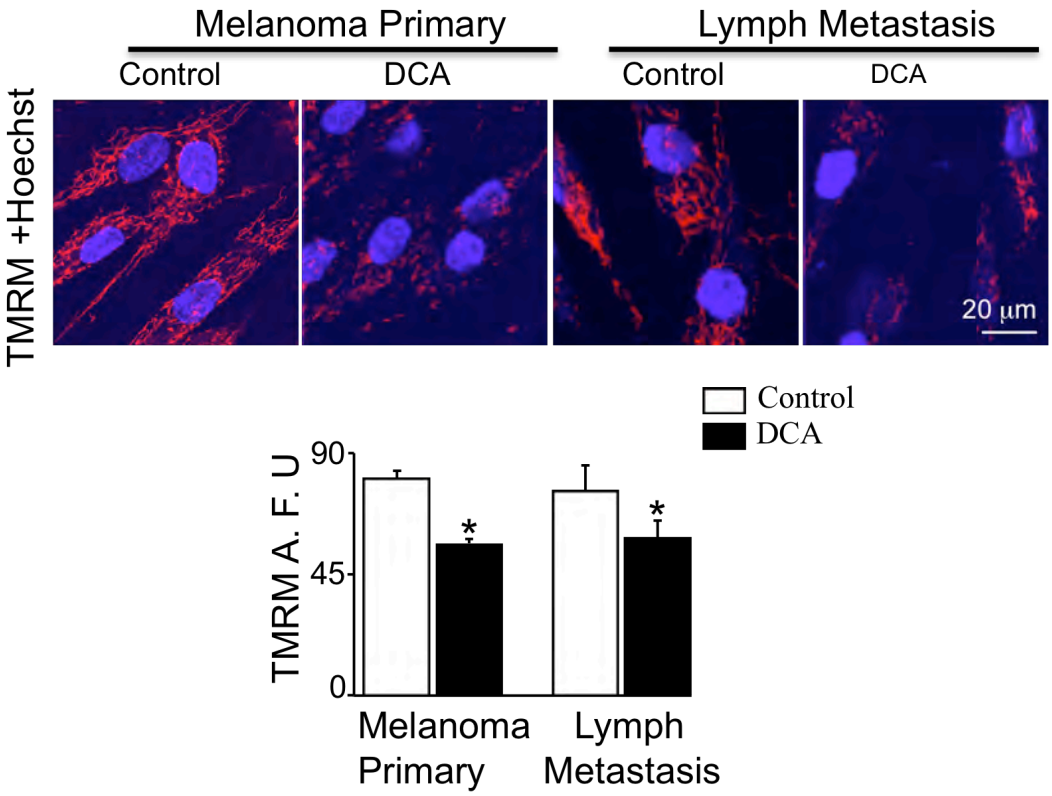

Figure 23: Comparison of DCA effects on ΔΨm in tumor cell lines developed from primary and metastatic (lymphatic) melanoma sites from the same patient.
Both cell lines have high Δψm and respond to DCA, suggesting that the ΔΨm effects of DCA can be studied in biopsy material from metastatic sites and perhaps be extrapolated to the primary tumor. N=50 P<0.05

Similarly, although baseline mROS production was not different between either of the primary or metastatic cell lines, DCA significantly increased mROS in both cell lines (Fig.24).

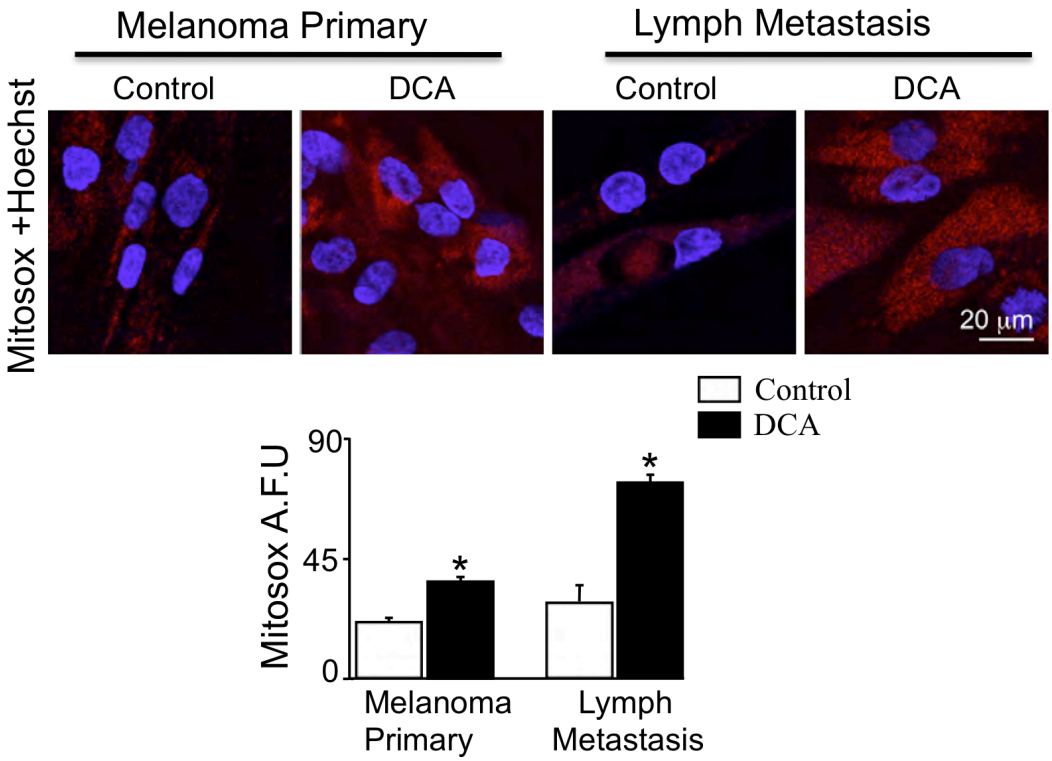

Figure 24: Comparison of DCA effects on mROS in tumor cell lines developed from primary and metastatic (lymphatic) melanoma sites from the same patient.
Both untreated cell lines have low ROS and respond to DCA treatment by increasing ROS. This suggests that the effect of DCA can be studied in biopsy material from metastatic sites and perhaps be extrapolated to the primary tumor. N=50 $P<0.05$

These results suggest that metabolic-targeting drugs like DCA may be beneficial for both primary and metastatic tumors. Similar results were also obtained when the primary colorectal adenocarcinoma was compared with its corresponding lymph node metastases and the effects of DCA on the ΔΨm (Fig.25) and mROS (Fig.26) on both cell types.

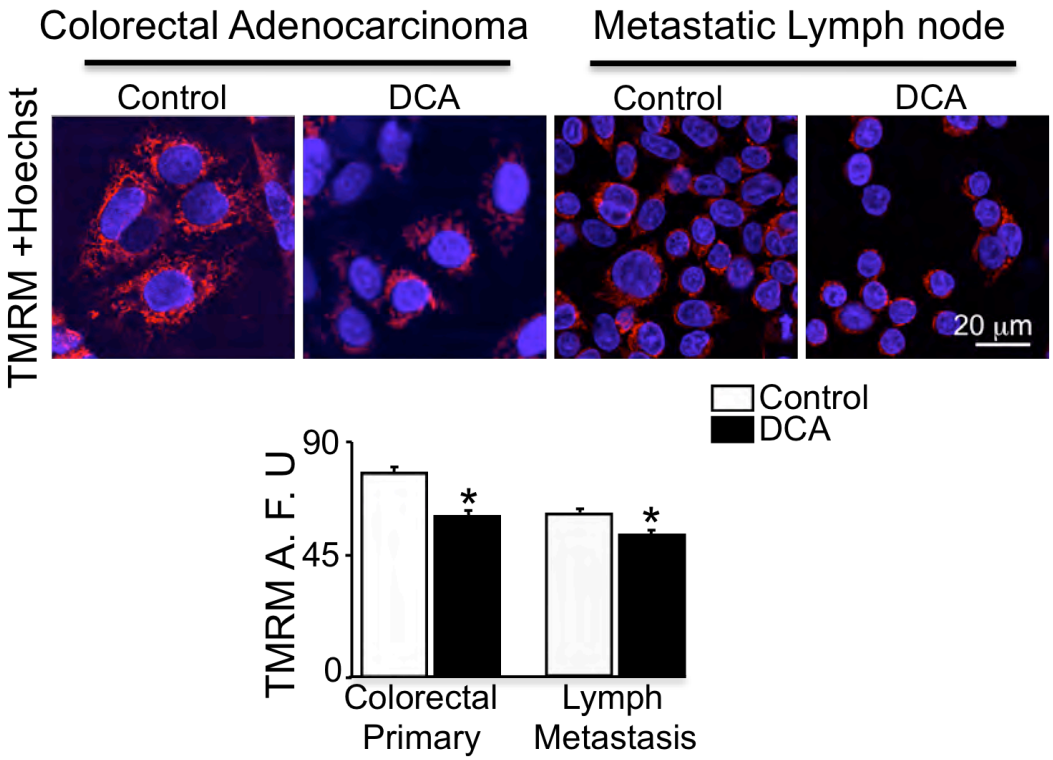

Figure 25: Comparison of DCA effects on ΔΨm in colorectal cancer versus metastasis. In contrast to Fig. 23, in this example the metastatic tumor cell lines show lower ΔΨm and respond less to DCA treatment compared to the primary tumor, suggesting a difference in the metabolic signaling upon metastasis. N=50 P<0.05

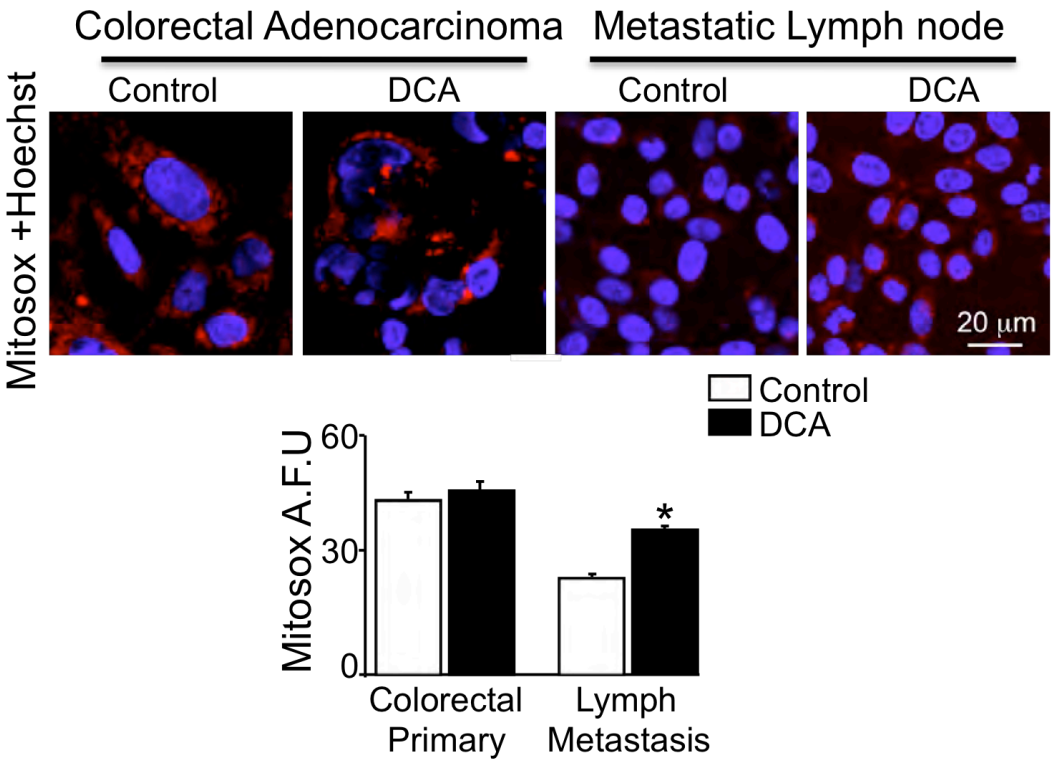

Figure 26: Comparison of DCA effects on mROS in colorectal cancer versus metastasis. In contrast to Fig. 24, in this example the primary tumor showed higher overall ROS. The metastatic tumor showed baseline ROS similar to Fig. 23. It responded more to DCA than the primary colorectal cells suggesting a difference in the metabolic signaling upon metastasis. N=50 $P<0.05$

Finally, it was assessed if confocal microscopy with live cell imaging could also be used to detect differences in $\Delta\Psi m$ and mROS in cell lines that express low and high levels of p53, a tumor suppressor protein that is mutated in many cancers. Mammary carcinoma cells expressing low levels of p53, had increased $\Delta\Psi m$ compared to mammary carcinoma cells expressing high levels of p53 (Fig. 27). DCA decreased $\Delta\Psi m$ in both cell lines, however, the effect of DCA was more pronounced in the mammary carcinoma cells expressing low levels of p53. Similarly, Mammary carcinoma cells expressing low levels of p53 had decreased mROS compared to mammary carcinoma cells expressing high levels of p53 with DCA increasing mROS in both cell lines (Fig. 28). In addition, mammary carcinoma cells expressing high levels of p53 had increased mROS compared to the p53 low expressing cells. These results are in keeping with recent work showing that p53 can upregulate mitochondrial function.

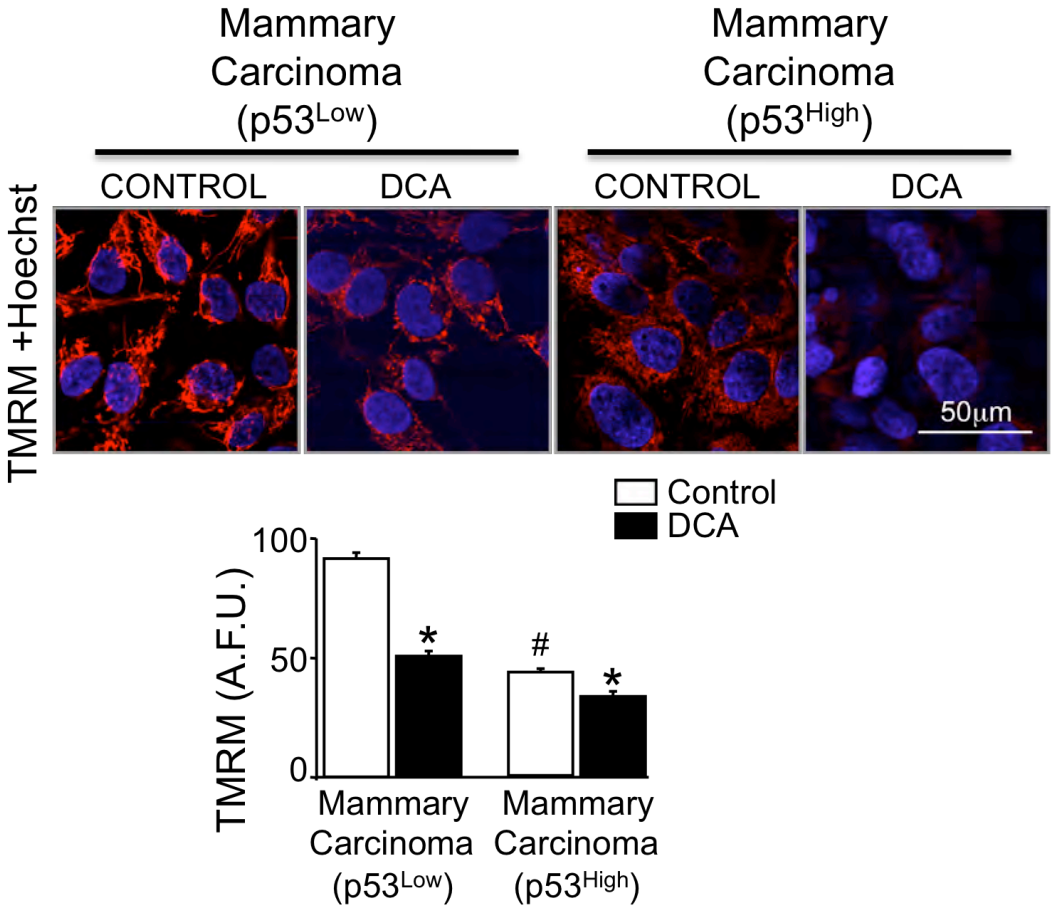

Figure 27: Comparison of DCA effects on ΔΨm between p53 high vs p53 low cells
An aggressive breast cancer line that has low levels of p53 is compared to a less aggressive breast caner line that has high levels of p53. Note that the aggressive tumor has much higher Δψm than the less aggressive tumor (and stronger response to DCA). This suggests that the degree of Δψm could predict the aggressiveness of the tumor. N=50 P<0.05

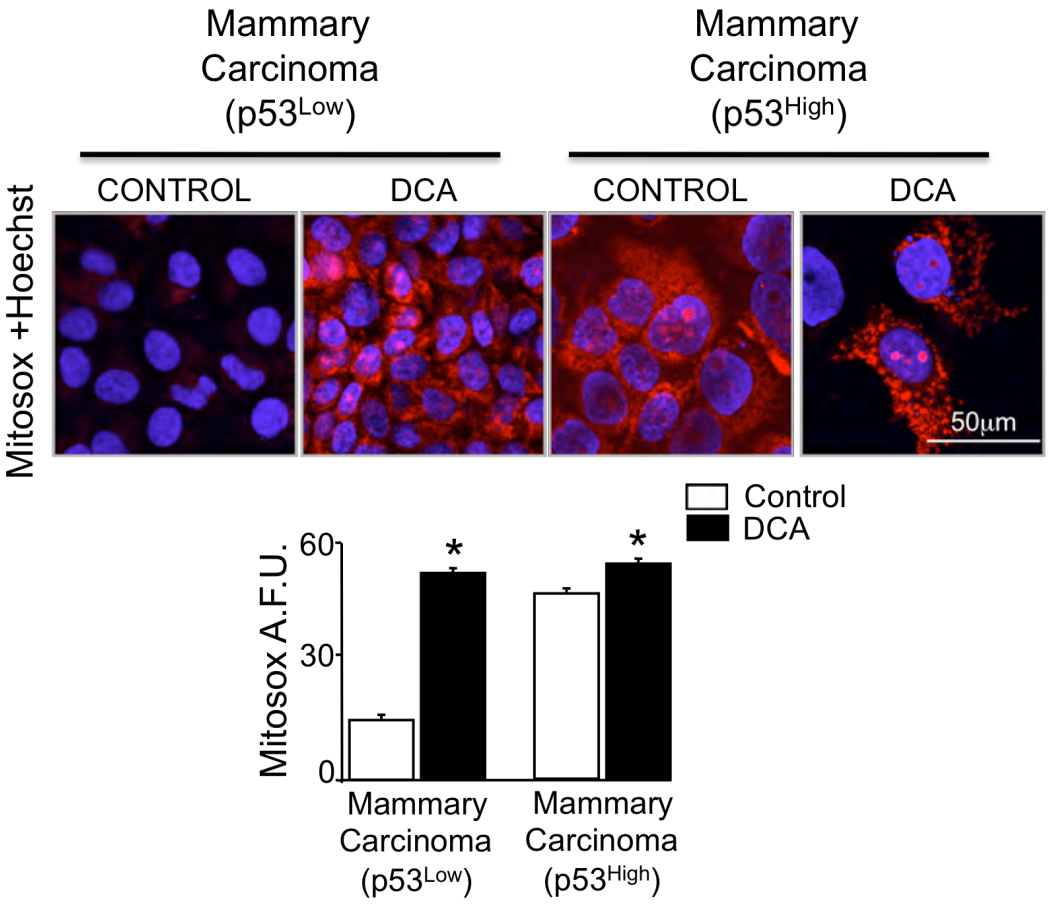

Figure 28: Comparison of DCA effects on mROS between p53 high vs p53 low cells
An aggressive breast cancer line that has low levels of p53 is compared to a less aggressive breast caner line that has high levels of p53. Note that the aggressive tumor has much lower ROS than the less aggressive tumor (and stronger response to DCA). This suggests that the degree of ROS could predict the aggressiveness of the tumor. N=50 $P<0.05$

Discussion

The fast biopsy has been the most commonly used method to diagnose the aggressiveness of tumors at the time of surgery. A tissue biopsy is collected by the surgeon and immediately sent to pathology for routine H&E staining and microscopic examination. The cell structure and boarders of the tumor in relation to the adjoining normal tissue are examined. If the tumor is invasive and has infiltrated the adjacent tissue the course of surgery may be altered to remove not only the tumor mass itself but also as much of the surrounding area as the surgeon deems necessary. While this technique is useful for determining the extent that a cancer has spread locally, at the time of surgery it is of limited value in making a prediction regarding a tumor's greater metastatic potential and responsiveness to other treatments such as chemotherapy. In this thesis representative and easily measurable biomarkers of possible tumor aggressiveness and potential response to non-surgical treatment were studied in an effort to provide a quick diagnosis of tumor aggressiveness and for treatment by metabolic modulating drugs like DCA.

For the purpose of my thesis I concentrated on certain functional biomarkers associated with the known glycolytic phenotype(*18*) and metabolic remodelling (*37*) of cancer cells. The biomarkers I chose to investigate were mitochondrial membrane voltage potential ($\Delta\psi m$) and mitochondrial reactive oxygen species (mROS). In order to determine whether these biomarkers can be used to assess the aggressiveness and treatment potential of cancers I performed functional analysis using the $\Delta\psi m$ indicator TMRM and the ROS indicator MITOSOX. I compared commercially available primary cancer cell lines, patient matched metastatic cells and patient matched normal cells. As well fresh glioblastoma tissue from biopsies obtained during debulking surgery was compared with "normal" (non-cancerous) brain tissue obtained during epilepsy surgery. The baseline differences between the levels of the chosen biomarkers were compared between the groups and correlated with the known phenotypes of the cells or tissue in question.

The results presented in this thesis show that confocal microscopy and live tissue/cell imaging with TMRM and MITOSOX can be used to assess mitochondrial function in GBM biopsies and various cancer cell lines, potentially allowing for quick prognosticative evaluation of the cancer. In addition it was shown that acute treatment with the PDK inhibitor DCA reversed the suppressed mitochondrial function (GO) observed in GBM tumor biopsies, suggesting that DCA may be a valid therapy for GBM

patients. When DCA was given to 5 patients with advanced GBM in a small clinical trial at the University of Alberta, it showed benefit (*1*).
These methods could be extended to other types of cancer and in other regions of the body and could be employed in conjunction with any tumor surgery or biopsy procedure.

Medical Implications for Diagnosis and Prognosis of Cancer:

Functional imaging of cancer cells is a potentially valuable technique for the diagnosis and prognosis of cancer. The correlation between elevated membrane potential of cancer mitochondria ($\Delta\psi m$) and resistance to apoptosis could be used as an indicator of the proliferative capacity and aggressiveness of many cancers (*52*), the higher the $\Delta\psi m$ is, the worse the potential outcome may be for the patient. The use of TMRM to measure $\Delta\psi m$ and Mitosox to measure reactive oxygen species (ROS) can give an indication of the aggressiveness of a cancer within a couple of hours of a live tumour biopsy becoming available to the confocal technician. In aggressive and highly proliferative cancers the mitochondrial membrane potential ($\Delta\psi m$) of the cancer cells as measured by TMRM staining is very high and the reactive oxygen species (ROS) as measured by MITOSOX is low. The cancer cells can also be cultured and various drug combinations can be tried in vitro to gauge their effect before any treatment is applied to the patient.

One limitation which might be encountered is that there may necessitate a time of trouble shooting of the technique to characterize it specifically for each type of cancer and to correlate the parameters measured ($\Delta\psi m$ and mROS) with the actual aggressiveness and response to treatment that is evidenced by experience. There would have to be close coordination with the operating team and the confocal technician to assure the viability and quality of the tissue being examined. This however should be a minor issue.

These techniques however, could be implemented immediately in any medical facility having ready access to a confocal microscope and qualified technician. The procedure for acquiring the tissue would be essentially identical to the fast biopsy procedure as it is now practiced. This would not require any changes in technique on the part of the surgeon, thus reducing any resistance which might be displayed toward the implementation of a new procedure.

REFERENCES

1. E. D. Michelakis *et al.*, *Sci Transl Med* **2**, 31ra34 (May 12, 2010).
2. C. Er, in *Techniques in microscopy for biomedical applications,* Schantz, Ed. (World Scientific Publishing Co. Pte. Ltd, 2006), vol. 2.
3. S. Inoue, in *Handbook of Biological Confocal Microscopy* J. B. Pawley, Ed. (Plenum Press, New York, 1995).
4. C. J. R. S. a. A. Choudhury, *Optica Acta: International Journal of Optics* **24**, 1051 (1977).
5. F. H. a. W. Denk, *Nature Methods* **2**, 932 (Dec 2005, 2005).
6. W. R. Zipfel, *Nature Biotechnology* **21**, 1369 (November 2003, 2003).
7. Zeiss, in *Carl Zeiss* (2003), pp. 1-30.
8. S.-W. Chu, *Microscopy research and technique* **66**, 193 (January 2005, 2005).
9. D. Kobat, *optics express* **17**, 13354 (20 07 2009, 2009).
10. Muller, *j microsc* **191**, 266 (1998).
11. D. P. a. W. W. Winfried Denk, in *Handbook of Biological Confocal Microscopy,* J. B. Pawley, Ed. (Plenum Press, New York, 1995), pp. 445-458.
12. R. Y. T. a. A. Waggoner, in *Handbook of Biological Microscopy,* J. B. Pawley, Ed. (Plenum Press, New York, 1995), pp. 267-279.
13. B. Alberts, in *Molecular Biology of the Cell,* B. Goatly, Ed. (Garlan Science, New York, 2008), pp. 813-876.
14. C. Borner, *Mol Immunol* **39**, 615 (Jan, 2003).
15. B. Alberts, in *Molecular Biology of the Cell,* B. Goatly, Ed. (Garland Science, New York, 2008).
16. A. C. Aisenberg, *Cancer Res* **21**, 304 (Apr, 1961).
17. F. Zhang, *j.mehy.*, 965 (Feb 2007, 2007).
18. Warburg, in *On metabolism of tumors*. (Constable, London, 1930).
19. R. A. Gatenby, R. J. Gillies, *Nat Rev Cancer* **4**, 891 (Nov, 2004).
20. P. Mitchell, J. Moyle, *Nature* **213**, 137 (Jan 14, 1967).
21. A. C. Aisenberg, *Cancer Res* **21**, 295 (Apr, 1961).
22. A. Isidoro, *Biochemical Journal* **378**, 17 (2004).
23. J.-w. Kim, *Cell Metabolism* **3**, 177 (2006).
24. P. Koivunen *et al.*, *J Biol Chem* **282**, 4524 (Feb 16, 2007).
25. E. D. Michelakis, L. Webster, J. R. Mackey, *Br J Cancer* **99**, 989 (Oct 7, 2008).
26. I. Papandreou, *Cell Metabolism* **3**, 187 (March 2006, 2006).
27. S. Abu-Hamad, H. Zaid, A. Israelson, E. Nahon, V. Shoshan-Barmatz, *J Biol Chem* **283**, 13482 (May 9, 2008).
28. M. Juhaszova, *The Journal of Clinical Investigation* **113**, 1535 (June 2004, 2004).
29. P. Liston, *Oncogene* **22**, 8568 (2003, 2003).
30. N. Majewski, *Mol Cell* **16**, 819 (03 12 2004, 2004).
31. L. Galluzzi, *Oncogene* **114**, 1 (2008).
32. L. Galluzzi, *Oncogene* **25**, 4812 (2006).
33. E. D. Michelakis, *Circulation* **117**, 2431 (2008, 2008).
34. P. W. Stacpoole, *Metabolism* **38**, 1124 (Nov, 1989).
35. M. M. Bowker-Kinley, W. I. Davis, P. Wu, R. A. Harris, K. M. Popov, *Biochem J* **329 (Pt 1)**, 191 (Jan 1, 1998).
36. T. R. Knoechel *et al.*, *Biochemistry* **45**, 402 (Jan 17, 2006).
37. S. Bonnet *et al.*, *Cancer Cell* **11**, 37 (Jan, 2007).
38. W. Cao *et al.*, *Prostate* **68**, 1223 (Aug 1, 2008).
39. I. Papandreou, T. Goliasova, N. C. Denko, *Int J Cancer*, (Oct 18, 2010).
40. M. Sanchez-Arago, M. Chamorro, J. M. Cuezva, *Carcinogenesis*, (Jan 15, 2010).
41. R. C. Sun *et al.*, *Breast Cancer Res Treat* **120**, 253 (Feb, 2010).
42. J. Y. Wong, G. S. Huggins, M. Debidda, N. C. Munshi, I. De Vivo, *Gynecol Oncol* **109**, 394 (Jun, 2008).
43. Y. Chen, R. Cairns, I. Papandreou, A. Koong, N. C. Denko, *PLoS One* **4**, e7033 (2009).

44. X. Yuan, *Oncogene* **23**, 9392 (2004).
45. I. Molecular Probes, *The Molecular Probes Handbook; A Guide to Fluorescent Probes and Labeling Technologies*. M. S. Iain Johnson, Ed., (Life Technologies, Carlsbad, CA, ed. Eleventh Edition, 2010), pp. 1060.
46. R. P. Haugland, Ed., *Handbook of Fluorescent Probes and Research Products*, (MOLECULAR PROBES Eugene, OR,USA, ed. 9, 2002), 9.
47. B. Ehrenberg, *Biophysical Journal* **53**, 785 (May 1988, 1988).
48. R. C. Scaduto, *Biophysical Journal* **76**, 469 (january 1999, 1999).
49. I. K. M. R. a. J. S. Beckman, *BioProbes* **53**, (July 2007, 2007).
50. K. M. Robinson *et al.*, *Proc Natl Acad Sci U S A* **103**, 15038 (Oct 10, 2006).
51. ABCAM, *abcam Protocols book*. (ed. first, 2011), pp. 90.
52. J. M. Cuezva, *Cancer research* **62**, 6674 (20 09 2002 2002).